TABLE 1—*Continued*

Accession no.	Symbol	Relative expression level (fold change)			Gene product
		S1T	MT-2	M8166	
NM_006509	I-REL	29.9 ± 3.0	65.0 ± 6.5	43.5 ± 5.1	Reticuloendotheliosis viral oncogene homolog B
AK096677	AK096677	29.2 ± 3.8	29.7 ± 7.2	73.3 ± 36.4	
NM_024758	FLJ23384	27.7 ± 4.5	23.1 ± 5.6	13.6 ± 2.1	Agmatine ureohydrolase (agmatinase)
AK021777	FLJ00205	25.8 ± 2.6	16.8 ± 1.7	19.9 ± 2.0	GalNAc transferase 10 isoform b
NM_001953	TP	25.2 ± 2.5	43.2 ± 4.3	30.8 ± 5.9	Endothelial cell growth factor 1 (platelet-derived)
NM_020731	AHH	24.8 ± 5.3	10.1 ± 1.6	99.4 ± 42.5	Arylhydrocarbon receptor repressor
NM_002413	GST2	24.6 ± 5.6	45.4 ± 4.6	51.5 ± 5.2	Microsomal glutathione *S*-transferase 2
NM_014383	Rog	24.3 ± 2.4	41.1 ± 4.1	12.5 ± 3.8	Testis zinc finger protein
NM_003928	MGC117411	24.2 ± 2.4	61.8 ± 7.1	35.8 ± 3.6	CAAX box 1
BX362492	BX362492	23.1 ± 4.0	26.3 ± 2.8	42.5 ± 11.0	
NM_033375	myr2	20.8 ± 2.9	45.4 ± 8.2	48.5 ± 8.3	Myosin IC
NM_213589	LPD	20.6 ± 2.3	14.9 ± 3.5	24.8 ± 3.1	Ras association and pleckstrin homology domains 1 isoform 2
NM_004838	HOMER-3	20.3 ± 2.0	193.6 ± 23.6	84.5 ± 15.8	Homer 3, neuronal immediate early gene
	A_23_P370707	18.2 ± 7.7	42.1 ± 4.2	30.1 ± 7.0	
AB033060	AHH	17.9 ± 3.9	12.2 ± 1.2	114.8 ± 22.4	Arylhydrocarbon receptor repressor
BC024020	VMP1	17.6 ± 2.6	39.6 ± 4.0	22.8 ± 6.0	Transmembrane protein 49
NM_023076	FLJ23360	17.6 ± 3.1	21.2 ± 4.0	20.5 ± 2.8	Hypothetical protein LOC65259
AK097976	DLEU2	17.2 ± 3.1	22.5 ± 5.3	13.6 ± 8.3	
NM_003842	DR5	16.7 ± 1.7	32.9 ± 4.0	37.2 ± 3.7	TNF receptor superfamily, member 10b isoform 1 precursor
NM_024646	ZYG11	16.5 ± 1.7	11.1 ± 1.1	15.1 ± 1.5	Zyg-11 homolog B
AK092921	HLA-B	16.3 ± 1.6	25.7 ± 2.6	19.9 ± 2.0	
NM_022152	RECS1	16.2 ± 1.6	13.6 ± 2.9	14.7 ± 3.0	Transmembrane BAX inhibitor motif containing 1
AA451906	BIN1	15.4 ± 1.5	18.2 ± 2.0	17.3 ± 1.7	
NM_018370	DRAM	15.3 ± 2.5	80.9 ± 14.7	41.6 ± 10.8	Damage-regulated autophagy modulator
NM_005514	HLA B	15.2 ± 1.7	32.3 ± 3.2	28.0 ± 4.9	MHC I, B
	THC2403644	14.9 ± 4.4	17.5 ± 5.9	15.0 ± 5.0	
NM_000152	LYAG	14.7 ± 1.5	15.8 ± 2.4	13.0 ± 2.1	Acid α-glucosidase preproprotein
	ENST00000355804	14.4 ± 1.4	23.7 ± 2.8	13.1 ± 1.7	
NM_001613	ACTSA	14.4 ± 1.6	35.3 ± 5.4	22.3 ± 2.3	α2 actin
NM_018370	DRAM	14.3 ± 2.3	73.3 ± 12.4	33.9 ± 7.7	Damage-regulated autophagy modulator
	A_24_P101771	14.0 ± 1.5	21.3 ± 2.2	19.3 ± 3.3	
NM_017789	SEMAI	13.9 ± 1.7	20.4 ± 2.5	33.9 ± 13.8	Semaphorin 4C
NM_002502	LYT10	13.3 ± 4.3	15.4 ± 1.0	45.9 ± 2.8	Nuclear factor of κ light polypeptide gene enhancer in B cells 2 (p49/p100)
NM_031419	IKBZ	12.6 ± 4.6	37.1 ± 4.9	134.0 ± 62.5	Nuclear factor of κ light polypeptide gene enhancer in B cells inhibitor, ζ isoform b
NM_015516	TSK	12.5 ± 1.2	12.7 ± 1.3	12.2 ± 1.2	Tsukushi
CR594843	HLA-B	12.2 ± 1.2	11.5 ± 1.2	10.1 ± 1.9	
NM_018950	HLAF	12.1 ± 1.8	16.7 ± 1.7	13.7 ± 2.0	MHC I, F precursor
NM_024567	PBHNF	12.0 ± 1.9	15.3 ± 3.0	17.0 ± 2.8	Homeobox containing 1
NM_003764	FHL4	12.0 ± 2.1	14.0 ± 1.4	11.7 ± 4.4	Syntaxin 11
	THC2276547	11.9 ± 1.3	16.8 ± 4.7	30.9 ± 9.6	
CA431756	CTTN	11.3 ± 1.4	13.8 ± 1.5	12.8 ± 3.1	
CR608347	HLA-B	11.0 ± 1.2	16.5 ± 1.4	12.7 ± 1.9	
NM_005261	KIR	11.0 ± 4.5	96.2 ± 9.6	97.3 ± 56.7	GTP-binding mitogen-induced T-cell protein
NM_130446	FLJ00029	11.0 ± 1.2	11.6 ± 3.5	13.6 ± 7.1	Kelch-like 6
NM_017789	SEMAI	10.9 ± 1.1	16.4 ± 1.6	24.6 ± 10.4	Semaphorin 4C
BC037255	LOC389634	10.6 ± 1.1	16.8 ± 3.0	21.3 ± 6.4	Hypothetical protein LOC389634
AF009619	CASH	10.6 ± 1.7	16.4 ± 3.3	85.1 ± 38.2	CASP8 and FADD-like apoptosis regulator
NM_006674	P5-1	10.5 ± 1.2	58.0 ± 5.8	91.4 ± 9.3	HLA complex P5
NR_001434	HLAHP	10.2 ± 1.0	15.7 ± 1.6	18.5 ± 2.4	

[a] The genes of which expression levels were more than 10-fold in all of the three HTLV-1-carrying T-cell lines (S1T, MT-2, and M8166) compared with the control T-cell line (MOLT-4) with statistical significance ($P < 0.05$) are listed and sorted by the expression level in S1T cells. All data represent means ± standard deviations for three independent microarray experiments.

high upregulation of the CD70 gene was reflected in the expression of the CD70 molecule on the surfaces of the cell lines.

CD70 expression in HTLV-1-carrying T-cell lines. As shown in Fig. 3, MOLT-4 cells did not express CD70 on their surfaces, whereas this molecule was highly expressed on the HTLV-1-carrying cell T-lines S1T, MT-2, M8166, and MT-4. Like the case for MOLT-4 cells, CD70 expression was scarcely observed for other HTLV-1-negative T-cell lines (CEM, Jurkat, and the monocytic cell lines U937 and HL-60), suggesting that CD70 is selectively expressed in HTLV-1-carrying T-cell lines. Such selectivity was also confirmed by the analysis of these cell lines for the expression of CD124, IL-21R, and CD151 on the surface. The gene expression of not only CD70 but also CD124, IL-21R, and CD151 was highly upregulated in all of the

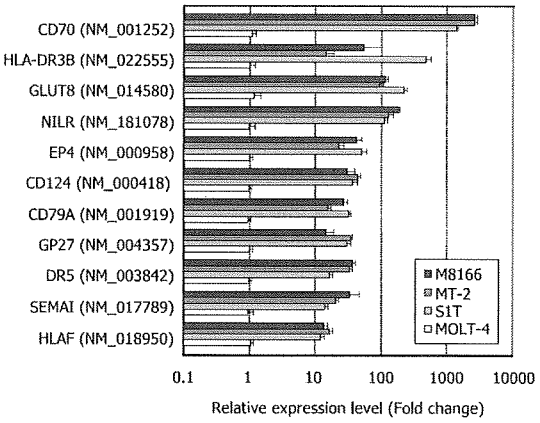

FIG. 2. Genes upregulated more than 10-fold in the HTLV-1-carrying T-cell lines S1T, MT-2, and M8166 compared with the genes in HTLV-1-negative T-cell line MOLT-4. The genes of which products are considered to be expressed on the cell surface are shown. All data represent means ± standard deviations (error bars) for three independent microarray experiments.

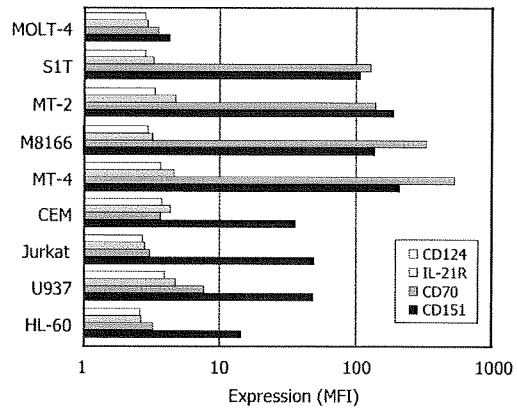

FIG. 4. Expression of CD124, IL-21R, CD70, and CD151 on various cell lines. The cells were strained with appropriate MAbs described in Materials and Methods and analyzed by laser flow cytometry. The expression level of each molecule is expressed as mean fluorescence intensity (MFI).

HTLV-1-carrying T-cell lines (Table 1 and Fig. 2). However, there was no significant difference of CD124 and IL-21R expression among the nine cell lines (Fig. 4). Like CD70, CD151 was strongly expressed on the HTLV-1-carrying T-cell lines compared with MOLT-4 cells, yet this molecule was also highly expressed on CEM, Jurkat, and U937 cells, indicating that CD151 expression was not selective enough to HTLV-1-carrying T-cell lines.

CD70 expression in leukemic cells from ATL patients. To determine whether CD70 is a potential target for anti-ATL

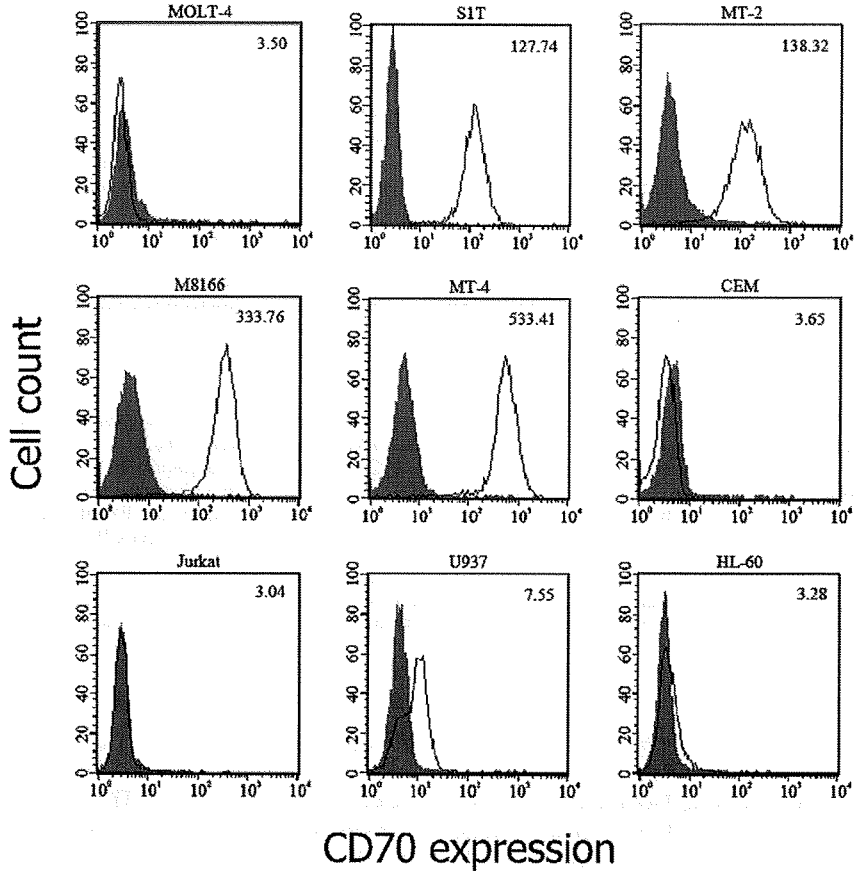

FIG. 3. CD70 expression on various cell lines. The cells were strained with an anti-human CD70 MAb (white histogram) or its isotype control MAb (gray histogram) and analyzed by laser flow cytometry. The number in each histogram indicates the mean fluorescence intensity of the cells.

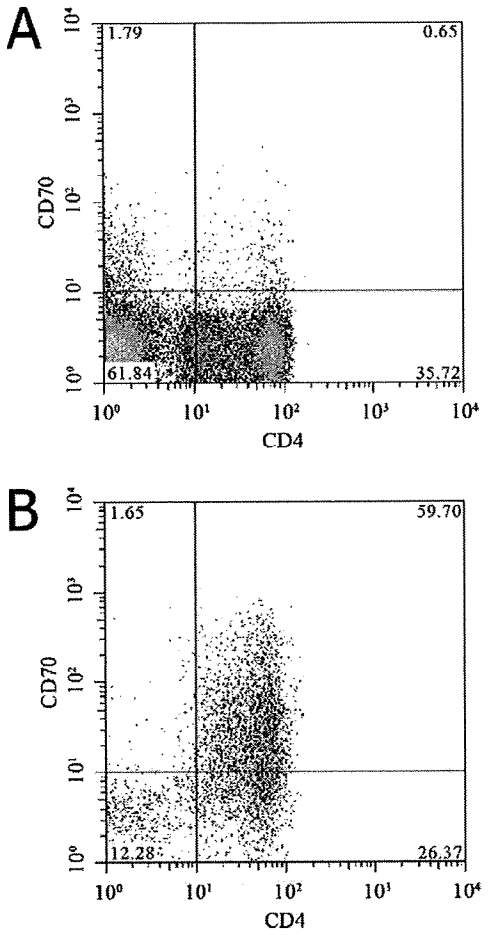

FIG. 5. CD70 expression on $CD4^+$ T cells isolated from healthy donors and ATL patients. PBMCs were isolated from (A) an HTLV-1-negative healthy donor (HD-1 in Table 1) and (B) an acute-type ATL patient (ATL-1 in Table 1). The cells were examined for their CD4 and CD70 expression by laser flow cytometry after being gated by their forward and side scattering intensities. The percentage of $CD70^+$ cells among $CD4^+$ cells was calculated by the following formula: percentage of upper right quadrant/(percentage of upper right quadrant + percentage of lower right quadrant).

MAb therapy, the selective expression of CD70 has to be demonstrated in the primary ATL cells isolated from patients. When PBMCs were isolated from an HTLV-1-negative healthy donor and examined for their CD4 and CD70 expression by laser flow cytometry, a small number (approximately 1.8%) of $CD4^+$ cells, which were regarded as T cells because of their being gated by forward and side scattering intensities, were $CD70^+$ (Fig. 5A). Under the same conditions, 69.2% of the $CD4^+$ cells isolated from an acute-type ATL patient were $CD70^+$ (Fig. 5B). Therefore, we extended the analysis to PBMCs obtained from an additional five HTLV-1-negative healthy donors and five acute-type ATL patients. As shown in Table 2, the average numbers of $CD70^+$ cells were 3.2 and 79.3% of the total $CD4^+$ T cells obtained from the healthy donors and ATL patients, respectively, which was statistically significant ($P < 0.00095$). In contrast, there was no practical difference of CD70 expression on B cells and monocytes between healthy donors and ATL patients. Although certain difference of CD70 expression was observed for $CD8^+$ T-cells, it was not statistically significant. Furthermore, difference of CD70 expression on $CD8^+$ T cells, B cells, and monocytes varied from one patient to another. These results suggest that CD70 is predominantly expressed on the $CD4^+$ T cells, presumably leukemia cells, from acute-type ATL patients.

Effect of anti-human CD70 MAb on ATL cells. When S1T and MOLT-4 cells were incubated with a commercially available anti-human CD70 MAb, the MAb did not affect the proliferation of these cell lines at a concentration of 1 μg/ml during a 4-day incubation period (Fig. 6A). The effect of an anti-human CD70 MAb for the viability of primary ATL cells was also examined. No significant reduction of cell viability was observed at concentrations of up to 1 μg/ml for all of the PBMCs obtained from three different ATL patients (Fig. 6B).

DISCUSSION

Human oligonucleotide microarrays have been used to examine gene expression patterns of PBMCs infected with HTLV-1 (11), HTLV-1-transformed T-cell lines (8, 30), Jurkat cells expressing either p12I (26) or p30II (23), and the Jurkat cell line JPX-9 that can be induced to express higher levels of Tax-1 (27). In addition, activated PBMC cDNA has been used in subtraction hybridization studies with cDNA from cultured ATL cells from a patient (33). The complexity of the data from these studies and differences in chip composition preclude a full definition of genes that are affected by viral infection. However, there is a consensus on the expression of some cellular genes. Enhanced expression of cell cycle and antiapoptotic genes includes the cyclin B1, p21WAF1/CIP1, and Bcl-X(L) genes, confirming prior biological/biochemical findings (1, 5, 25, 28). In contrast, caspase-8 appears to be consistently downregulated. Among the interleukins and their receptors, the upregulation of IL-2Rα, but not IL-2, is also consistently detected. In contrast, IL-15Rα appears to be upregulated in only some HTLV-1-infected T-cell lines and PBMCs. Similarly, IL-15 is not upregulated in all cell lines and IL-15 expression does not appear to be induced by Tax-1 in Jurkat cells.

There is a criticism that limited or biased information regarding the molecules selectively expressed in ATL cells will be obtained when HTLV-1-carrying T-cell lines, instead of primary ATL cells, are used for oligonucleotide microarray analysis (35). This criticism may be appropriate from one aspect, since such HTLV-1-carrying T-cell lines generally express the viral transactivator protein Tax that considerably affects viral and cellular gene expression. In fact, our study demonstrated that MT-2 and M8166 cells strongly expressed Env-Tax fusion protein and Tax, respectively (Fig. 1B). Both cell lines were established by cocultivation of healthy human cord blood T cells with ATL cells (24). Therefore, it is not surprising that unlike primary ATL cells, these in vitro-transformed T-cell lines still retain functional Tax. This may be a reason for the high correlation coefficient (0.96) in relative expression levels of the 108 genes between MT-2 and M8166 cells (Table 1). On the other hand, S1T cells were directly established from primary ATL cells by cultivation with IL-2 (2). Consequently, S1T cells did not express *env* or *tax* gene as well as Env or Tax (Fig. 1).

TABLE 2. CD70 expression in PBMCs isolated from healthy donors and ATL patients[a]

Donor	WBC[b] (cells/mm^3)	Expression on indicated marker-positive cells (%)[c]						
		$CD3^+$ $CD70^+$	$CD4^+$ $CD70^+$	$CD4^+$ $CD25^+$	$CD4^+$ $CD25^+$ $CD70^+$	$CD8^-$ $CD70^+$	$CD19^+$ $CD70^+$	$CD14^+$ $CD70^+$
HD-1		2.6	1.8	ND	0.3	0.6	16.5	0
HD-2		2.9	2.7	1.5	0.4	4.2	17.9	0.1
HD-3		2.4	1.9	3.6	0.4	0.2	13.6	0
HD-4		6.3	4.2	7.1	1.2	0.6	20.3	0.5
HD-5		9.4	5.8	7.7	1.3	3.9	15.8	0.3
HD-6		5.5	2.8	14.2	1.3	ND	27.5	0.3
ATL-1	414,000	67.5	69.2	73.6	56.6	ND	14.5	0
ATL-2	28,300	98.0	98.6	97.5	98.5	91.3	18.3	0
ATL-3	296,000	66.6	84.3	40.6	36.9	0	0	0
ATL-4	9,100	99.1	98.7	58.7	58.8	84.6	8.7	0.5
ATL-5		81.6	31.5	10.4	5.7	74.6	21.5	33.9
ATL-6		94.3	93.4	73.1	69.6	24.5	16.7	1.5

[a] PBMCs obtained from healthy donors (HD) and acute-type ATL patients were stained with appropriate MAbs (see Materials and Methods). After staining, the cells were analyzed by laser flow cytometry.

[b] WBC, white blood cell count.

[c] Mean ± standard deviation values for healthy donors were 4.9 ± 2.8 for $CD3^+$ $CD70^+$ cells, 3.2 ± 1.5 for $CD4^+$ $CD70^+$ cells, 6.8 ± 4.8 for $CD4^+$ $CD25^+$ cells, 0.8 ± 0.5 for $CD4^+$ $CD25^+$ $CD70^+$ cells, 1.9 ± 2.0 for $CD8^+$ $CD70^+$ cells, 18.6 ± 4.9 for $CD19^+$ $CD70^+$ cells, and 0.2 ± 0.2 for $CD14^+$ $CD70^+$ cells. Mean ± standard deviation values for ATL patients were 84.5 ± 14.9 for $CD3^+$ $CD70^+$ cells (statistically significant [$P < 0.01$] by t test), 79.3 ± 25.9 for $CD4^+$ $CD70^+$ cells (statistically significant [$P < 0.01$] by t test), 59.0 ± 30.3 for $CD4^+$ $CD25^+$ cells (statistically significant [$P < 0.01$] by t test), 54.4 ± 31.2 for $CD4^+$ $CD25^+$ $CD70^+$ cells (statistically significant [$P < 0.01$] by t test), 55.0 ± 40.4 for $CD8^+$ $CD70^+$ cells, 13.3 ± 7.8 for $CD19^+$ $CD70^+$ cells, and 6.0 ± 13.7 for $CD14^+$ $CD70^+$ cells. ND, not determined.

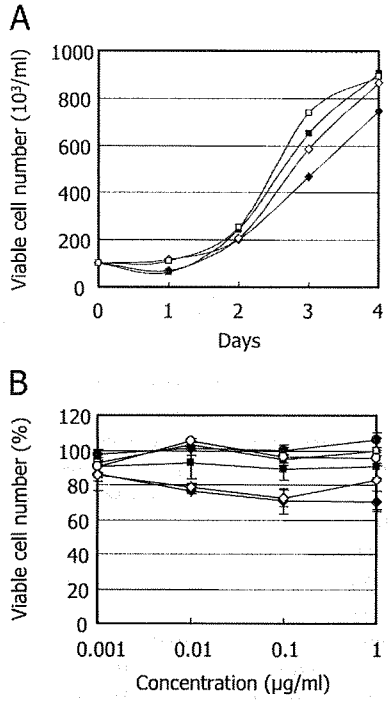

FIG. 6. Effect of anti-human CD70 MAb on the growth and viability of ATL cells. (A) S1T (diamonds) and MOLT-4 (squares) cells were incubated with an anti-CD70 MAb (filled symbols) or its isotype-matched control MAb (open symbols) at a concentration of 1 μg/ml. After a 4-day incubation, the number of viable cells was determined by trypan blue exclusion. (B) PBMCs obtained from three different ATL patients (circles, squares, and diamonds) were incubated with an anti-CD70 MAb (closed symbols) or its isotype-matched control MAb (open symbols) at various concentrations. After a 24-h incubation, the number of viable cells was determined by the MTT method. Error bars indicate standard deviations.

In this point of view, if HTLV-1-carrying T-cell lines with totally different origins could be included for oligonucleotide microarray analysis, it would become an efficient approach to determining the molecules selectively expressed in ATL cells. In the present study, 108 genes were found to be upregulated more than 10-fold in different HTLV-1-carrying T-cell lines relative to a control T-cell line (Table 1). Among them, tremendous (more than 1,000-fold) upregulation was observed for the CD70 gene, of which product should be expressed on the cell surface (Fig. 2). In fact, the CD70 molecule was strongly and selectively expressed on various HTLV-1-carrying T-cell lines and $CD4^+$ T-cells obtained from ATL patients but not on HTLV-1-negative T-cell lines, monocytic cell lines, or $CD4^+$ T-cells obtained from HTLV-1-negative healthy donors (Fig. 4 and 5 and Table 2).

CD70 is the only known ligand for its receptor CD27 that belongs to the TNF receptor superfamily 7. In general, this molecule is expressed on strongly activated T and B cells (4) and some hematological malignancies, such as non-Hodgkin's lymphoma (42). In fact, when PBMCs were isolated and stimulated with phytohemagglutinin, approximately 18 and 32% of the cells became $CD70^+$ after 7 and 12 days of cultivation, respectively (data not shown). However, there has been no definitive report describing the selective expression of CD70 in ATL cells. CD70 is also highly expressed on some solid tumors, including renal cell carcinoma (9, 17) and glioblastoma (6, 43). In contrast, CD70 expression is highly restricted in normal tissues (19). Therefore, CD70 has been considered to be an attractive target of MAbs and MAb-drug conjugates for selective anticancer therapy. It was recently shown that the administration of an engineered anti-CD70 MAb significantly prolonged the survival of severe combined immunodeficient mice bearing $CD70^+$-disseminated human non-Hodgkin's lymphoma xenografts (22). In this study, treatment with control IgG did not prolong median survival (21 days). In contrast, median survival was increased to 72 days when the mice were

treated with the anti-CD70 MAb at a dose of 4 mg/kg of body weight. Furthermore, anti-CD70 antibody-drug conjugates were effective against tumor growth in mice bearing human renal cell carcinoma xenografts (6). These results suggest that irrespective of drug conjugates, anti-CD70 MAbs deserve to be investigated for their anticancer activities against ATL in vitro and in vivo.

In addition to CD70, we have also identified 10 genes of which products should be highly expressed on the HTLV-1-carrying T-cell lines (Fig. 2). Among these, three molecules, CD124, IL-21R, and CD151, could be evaluated for their expressions on various cell lines, since MAbs for these molecules were commercially available. CD151 was indeed highly expressed on the HTLV-1-carrying T-cell lines, yet it was also expressed in other T-cell and monocytic cell lines, except MOLT-4 (Fig. 4). CD151 is a member of the tetraspanin family and is a broadly expressed molecule. It is also noted for its strong molecular associations with integrins (44). CD151 was initially identified as a marker of human acute myeloid leukemia cells, platelets, and vascular endothelial cells (3). The upregulation of the CD151 gene in HTLV-1-carrying T-cell lines has already been reported and investigated for its pathological role (13, 14). Our microarray analysis has confirmed these reports. Since CD151 is broadly expressed by a variety of cell types (36), it does not seem to be a suitable target for anticancer therapy with MAbs. Further studies are in progress to identify other molecules selectively expressed on primary ATL cells obtained from patients.

At present, there is no evidence indicating that commercially available anti-CD70 MAbs are capable of inhibiting cell proliferation or inducing apoptosis of primary ATL cells obtained from patients as well as the S1T cells (Fig. 6). It is possible that these anti-CD70 MAbs are not optimized to exert their biological functions and may be required for structural modification. However, a company in New Jersey has recently obtained permission from the U.S. Food and Drug Administration to use a fully human MAb directed against CD70 in a phase I clinical trial for treatment of clear cell renal cell carcinoma (Medarex). Considering this fact and the poor prognosis and lack of curative therapy for ATL, CD70 should be further perused as a potential target in anticancer therapy against ATL.

ACKNOWLEDGMENTS

The anti-p40 Tax monoclonal antibody Lt-4 was kindly provided by Y. Tanaka (University of the Ryukyus, Okinawa, Japan). We thank T. Uto and M. Tokitou for their technical assistance.

This work was supported by a grant from the Frontier Science Research Center, Kagoshima University, and a grant-in-aid for Scientific Research (B) from the Japan Society for the Promotion of Science (grant no. 19390153).

REFERENCES

1. **Akagi, T., H. Ono, and K. Shimotohno.** 1996. Expression of cell-cycle regulatory genes in HTLV-I infected T-cell lines: possible involvement of Tax1 in the altered expression of cyclin D2, p18(Ink4) and p21(Waf1/Cip1/Sdi1). Oncogene **12**:1645–1652.
2. **Arima, N., J. A. Molitor, M. R. Smithe, J. H. Kim, Y. Daitoku, and W. C. Greene.** 1991. Human T-cell leukemia virus type I Tax induces expression of the Rel-related family of κB enhancer-binding proteins: evidence for a pretranslational component of regulation. J. Virol. **65**:6892–6899.
3. **Ashman, L. K., G. Aylett, P. Mehrabani, L. Bendall, S. Niutta, A. C. Cambareri, S. R. Cole, and M. Berndt.** 1991. The murine monoclonal antibody, 14A2.H1, identifies a novel platelet surface antigen. Br. J. Haematol. **79**:263–270.
4. **Borst, J., J. Hendriks, and Y. Xiao.** 2005. CD27 and CD70 in T cell and B cell activation. Curr. Opin. Immunol. **17**:275–281.
5. **Cereseto, A., J. C. Mulloy, and G. Franchini.** 1996. Insights on the pathogenicity of human T-lymphotropic/leukemia virus types I and II. J. Acquir. Immune Defic. Syndr. Hum. Retrovirol. **13**(Suppl. 1):S69–S75.
6. **Chahlavi, A., P. Rayman, A. L. Richmond, K. Biswas, R. Zhang, M. Vogelbaum, C. Tannenbaum, G. Barnett, and J. H. Finke.** 2005. Glioblastomas induce T-lymphocyte death by two distinct pathways involving gangliosides and CD70. Cancer Res. **65**:5428–5438.
7. **Choi, Y. L., K. Tsukasaki, M. C. O'Neill, Y. Yamada, Y. Onimaru, K. Matsumoto, J. Ohashi, Y. Yamashita, S. Tsutsumi, R. Kaneda, S. Takada, H. Aburatani, S. Kamihira, T. Nakamura, M. Tomonaga, and H. Mano.** 2007. A genomic analysis of adult T-cell leukemia. Oncogene **26**:1245–1255.
8. **de La Fuente, C., L. Deng, F. Santiago, L. Arce, L. Wang, and F. Kashanchi.** 2000. Gene expression array of HTLV type 1-infected T cells: up-regulation of transcription factors and cell cycle genes. AIDS Res. Hum. Retrovir. **16**:1695–1700.
9. **Diegmann, J., K. Junker, B. Gerstmayer, A. Bosio, W. Hindermann, J. Rosenhahn, and F. von Eggeling.** 2005. Identification of CD70 as a diagnostic biomarker for clear cell renal cell carcinoma by gene expression profiling, real-time RT-PCR and immunohistochemistry. Eur. J. Cancer **41**:1794–1801.
10. **Gessain, A., F. Barin, J. C. Vernant, O. Gout, L. Maurs, A. Calender, and G. de Thé.** 1985. Antibodies to human T-lymphotropic virus type-I in patients with tropical spastic paraparesis. Lancet **2**:407–410.
11. **Harhaj, E. W., L. F. Good, G. T. Xiao, and S. C. Sun.** 1999. Gene expression profiles in HTLV-I-immortalized T cells: deregulated expression of genes involved in apoptosis regulation. Oncogene **18**:1341–1349.
12. **Harris, M.** 2004. Monoclonal antibodies as therapeutic agents for cancer. Lancet Oncol. **5**:292–302.
13. **Hasegawa, H., Y. Utsunomiya, K. Kishimoto, K. Yanagisawa, and S. Fujita.** 1996. SFA-1, a novel cellular gene induced by human T-cell leukemia virus type 1, is a member of the transmembrane 4 superfamily. J. Virol. **70**:3258–3263.
14. **Hasegawa, H., T. Nomura, K. Kishimoto, K. Yanagisawa, and S. Fujita.** 1998. SFA-1/PETA-3 (CD151), a member of the transmembrane 4 superfamily, associates preferentially with $\alpha_5\beta_1$ integrin and regulates adhesion of human T cell leukemia virus type 1-infected T cells to fibronectin. J. Immunol. **161**:3087–3095.
15. **Iannello, A., and A. Ahmad.** 2005. Role of antibody-dependent cell-mediated cytotoxicity in the efficacy of therapeutic anti-cancer monoclonal antibodies. Cancer Metastasis Rev. **24**:487–499.
16. **Ishikawa, T.** 2003. Current status of therapeutic approaches to adult T-cell leukemia. Int. J. Hematol. **78**:304–311.
17. **Junker, K., W. Hindermann, F. von Eggeling, J. Diegmann, K. Haessler, and J. Schubert.** 2005. CD70: a new tumor specific biomarker for renal cell carcinoma. J. Urol. **173**:2150–2153.
18. **Kobayashi, N., H. Konishi, H. Sabe, K. Shigesada, T. Noma, T. Honjo, and M. Hatanaka.** 1984. Genomic structure of HTLV (human T-cell leukemia virus): detection of defective genome and its amplification in MT-2 cells. EMBO J. **3**:1339–1343.
19. **Law, C. L., K. A. Gordon, B. E. Toki, A. K. Yamane, M. A. Hering, C. G. Cerveny, J. M. Petroziello, M. C. Ryan, L. Smith, R. Simon, G. Sauter, E. Oflazoglu, S. O. Doronina, D. L. Meyer, J. A. Francisco, P. Carter, P. D. Senter, J. A. Copland, C. G. Wood, and A. F. Wahl.** 2006. Lymphocyte activation antigen CD70 expressed by renal cell carcinoma is a potential therapeutic target for anti-CD70 antibody-drug conjugates. Cancer Res. **66**:2328–2337.
20. **Lin, M. Z., M. A. Teitell, and G. J. Schiller.** 2005. The evolution of antibodies into versatile tumor-targeting agents. Clin. Cancer Res. **11**:129–138.
21. **Marcus, R., and A. Hagenbeek.** 2007. The therapeutic use of rituximab in non-Hodgkin's lymphoma. Eur. J. Haematol. S. **67**:5–14.
22. **McEarchern, J. A., E. Oflazoglu, L. Francisco, C. F. McDonagh, K. A. Gordon, I. Stone, K. Klussman, E. Turcott, N. van Rooijen, P. Carter, I. S. Grewal, A. F. Wahl, and C. L. Law.** 2007. Engineered anti-CD70 antibody with multiple effector functions exhibits in vitro and in vivo antitumor activities. Blood **109**:1185–1192.
23. **Michael, B., A. M. Nair, H. Hiraragi, L. Shen, G. Feuer, K. Boris-Lawrie, and M. D. Lairmore.** 2004. Human T lymphotropic virus type-1 p30II alters cellular gene expression to selectively enhance signaling pathways that activate T lymphocytes. Retrovirology **1**:39.
24. **Miyoshi, I., I. Kubonishi, S. Yoshimoto, T. Akagi, Y. Ohtsuki, Y. Shiraishi, K. Nagata, and Y. Hinuma.** 1981. Type C virus particles in a cord T-cell line derived by co-cultivating normal human cord leukocytes and human leukaemic T cells. Nature **294**:770–771.
25. **Mori, N., M. Fujii, G. Cheng, S. Ikeda, Y. Yamasaki, Y. Yamada, M. Tomonaga, and N. Yamamoto.** 2001. Human T-cell leukemia virus type I tax protein induces the expression of anti-apoptotic gene Bcl-xL in human T-cells through nuclear factor-κB and c-AMP responsive element binding protein pathways. Virus Genes **22**:279–287.
26. **Nair, A., B. Michael, H. Hiraragi, S. Fernandez, G. Feuer, K. Boris-Lawrie, and M. Lairmore.** 2005. Human T lymphotropic virus type 1 accessory protein p12I modulates calcium-mediated cellular gene expression and enhances p300 expression in T lymphocytes. AIDS Res. Hum. Retrovir. **21**:273–284.

27. **Ng, P. W., H. Iha, Y. Iwanaga, M. Bittner, Y. Chen, Y. Jiang, G. Gooden, J. M. Trent, P. Meltzer, K. T. Jeang, and S. L. Zeichner.** 2001. Genome-wide expression changes induced by HTLV-1 Tax: evidence for MLK-3 mixed lineage kinase involvement in Tax-mediated NF-κB activation. Oncogene **20**:4484–4496.
28. **Nicot, C., R. Mahieux, S. Takemoto, and G. Franchini.** 2000. Bcl-X(L) is up-regulated by HTLV-I and HTLV-II in vitro and in ex vivo ATLL samples. Blood **96**:275–281.
29. **Osame, M., K. Usuku, S. Izumo, N. Ijichi, H. Amitani, A. Igata, M. Matsumoto, and M. Tara.** 1986. HTLV-I associated myelopathy, a new clinical entity. Lancet **1**:10310–11032.
30. **Pise-Masison, C. A., M. Radonovich, R. Mahieux, P. Chatterjee, C. Whiteford, J. Duvall, C. Guillerm, A. Gessain, and J. N. Brady.** 2002. Transcription profile of cells infected with human T-cell leukemia virus type I compared with activated lymphocytes. Cancer Res. **62**:3562–3571.
31. **Proietti, F. A., A. B. Carneiro-Proietti, B. C. Catalan-Soares, and E. L. Murphy.** 2005. Global epidemiology of HTLV-I infection and associated diseases. Oncogene **24**:6058–6068.
32. **Reff, M. E., K. Carner, K. S. Chambers, P. C. Chinn, J. E. Leonard, R. Raab, R. A. Newman, N. Hanna, and D. R. Anderson.** 1994. Depletion of B cells in vivo by a chimeric mouse human monoclonal antibody to CD20. Blood **83**:435–445.
33. **Ruckes, T., D. Saul, J. Van Snick, O. Hermine, and R. Grassmann.** 2001. Autocrine antiapoptotic stimulation of cultured adult T-cell leukemia cells by overexpression of the chemokine I-309. Blood **98**:1150–1159.
34. **Salahuddin, S. Z., P. D. Markham, F. Wong-Staal, G. Franchini, V. S. Kalyanaraman, and R. C. Gallo.** 1983. Restricted expression of human T-cell leulemia-lymphoma virus (HTLV) in transformed human umbilical cord blood lymphocytes. Virology **129**:51–64.
35. **Sasaki, H., I. Nishikata, T. Shiraga, E. Akamatsu, T. Fukami, T. Hidaka, Y. Kubuki, A. Okayama, K. Hamada, H. Okabe, Y. Murakami, H. Tsubouchi, and K. Morishita.** 2005. Overexpression of a cell adhesion molecule, TSLC1, as a possible molecular marker for acute-type adult T-cell leukemia. Blood **105**:1204–1213.
36. **Sincock, P., G. Mayrhofer, and L. K. Ashman.** 1997. Localization of the transmembrane 4 superfamily (TM4SF) member PETA-3 (CD151) in normal human tissues: comparison with CD9, CD63, and α5β1 integrin. J. Histochem. Cytochem. **45**:515–525.
37. **Takatsuki, K.** 2005. Discovery of adult T-cell leukemia. Retrovirology **2**:16.
38. **Tanaka, Y., A. Yoshida, Y. Takayama, H. Tsujimoto, A. Tsujimoto, M. Hayami, and H. Tozawa.** 1990. Heterogeneity of antigen molecules recognized by anti-tax1 monoclonal antibody Lt-4 in cell lines bearing human T cell leukemia virus type I and related retroviruses. Jpn. J. Cancer Res. **81**:225–231.
39. **Taylor, G. P., and M. Matsuoka.** 2005. Natural history of adult T-cell leukemia/lymphoma and approaches to therapy. Oncogene **24**:6047–6057.
40. **Uchiyama, T., J. Yodoi, K. Sagawa, K. Takatsuki, and H. Uchino.** 1977. Adult T-cell leukemia: clinical and hematologic features of 16 cases. Blood **50**:481–492.
41. **Wang, X., H. Miyake, M. Okamoto, M. Saito, J. Fujisawa, Y. Tanaka, S. Izumo, and M. Baba.** 2002. Inhibition of the tax-dependent human T-lymphotropic virus type I replication in persistently infected cells by the fluoroquinolone derivative K-37. Mol. Pharmacol. **61**:1359–1365.
42. **Widney, D., G. Gundapp, J. W. Said, M. van der Meijden, B. Bonavida, A. Demidem, C. Trevisan, J. Taylor, R. Detels, and O. Martinez-Maza.** 1999. Aberrant expression of CD27 and soluble CD27 (sCD27) in HIV infection and in AIDS-associated lymphoma. Clin. Immunol. **93**:114–123.
43. **Wischhusen, J., G. Jung, I. Radovanovic, C. Beier, J. P. Steinbach, A. Rimner, H. Huang, J. B. Schulz, H. Ohgaki, A. Aguzzi, H. G. Rammensee, and M. Weller.** 2002. Identification of CD70-mediated apoptosis of immune effector cells as a novel immune escape pathway of human glioblastoma. Cancer Res. **62**:2592–2599.
44. **Wright, M. D., S. M. Geary, S. Fitter, G. W. Moseley, L. M. Lau, K. C. Sheng, V. Apostolopoulos, E. G. Stanley, D. E. Jackson, and L. K. Ashman.** 2004. Characterization of mice lacking the tetraspanin superfamily member CD151. Mol. Cell. Biol. **24**:5978–5988.

J. Biochem. **143,** 833–839 (2008)
doi:10.1093/jb/mvn038

One-Step Purification of Lectins from Banana Pulp Using Sugar-Immobilized Gold Nano-Particles

Sachiko Nakamura-Tsuruta[1], Yuko Kishimoto[3], Tomoaki Nishimura[3] and Yasuo Suda[1,2,3,*]

[1]Venture Business Laboratory; [2]Department of Nanostructure and Advanced Materials, Kagoshima University, 1-21-40, Kohrimoto, Kagoshima 890-0065; and [3]SUDx-Biotec Corp., KIBC #461, 5-5-2, Minatojima-minami, Chuo-ku, Kobe 650-0047, Japan

Received December 24, 2007; accepted February 29, 2008; published online March 15, 2008

To obtain lectins without tedious purification steps, we developed a convenient method for a one-step purification of lectins using sugar-immobilized gold nano-particles (SGNPs). Proteins in crude extracts from plant materials were precipitated with 60% ammonium sulphate, and the precipitate was re-dissolved in a small volume of phosphate buffer. The resultant solution was then mixed with appropriate SGNPs under an optimized condition. After incubating overnight at 4°C, lectins in the mixture formed aggregate with SGNPs, which was visually detected and easily sedimented by centrifugation. The aggregate was dissolved by adding inhibitory sugars, which were identical to the non-reducing sugar moieties on the SGNPs. According to SDS–PAGE and MS of thus obtained proteins, it was found that SGNPs isolated lectins with a high purity. For example, a protein isolated from banana using Glcα-GNP (α-glucose-immobilized gold nano-particle) was identified as banana lectin by trypsin-digested peptide-MS finger printing method.

Key words: gold nano particle, lectin, peptide MS fingerprinting, purification, sugar chain.

Abbreviations: CHCA, α-cyano-4-hydroxycinnamic acid; Glcα-GNP, alpha-glucose-immobilized gold nano-particle; GlcNAcα-GNP, alpha-*N*-acetyl-glucosamine-immobilized gold nano-particle; Manα-GNP, alpha-mannose-immobilized gold nano-particle; SA, 3,5-dimethyl-4-hydroxycinnamic acid; SGNPs, sugar-immobilized gold nano-particles.

Lectins are carbohydrate-binding proteins, which can specifically recognize sugar structures (*1*). Their physiological functions have been argued for a long time, and were recently determined for several lectins. Selectins mediate the adhesion of leucocytes and the endothelial cells of blood vessels. Some plant lectins serve as defence factors against phytopathogenic fungi, insect and animals by interacting with their glycans (*2–4*). According to these examples, lectin–glycan interactions are recognized as important in biological processes in both plant and animal bodies. To understand the functions of lectins at the molecular level in detail, purification and subsequent characterization are the most crucial.

To purify lectins from crude extract, several chromatography techniques, such as affinity chromatography, ion-exchange chromatography and gel permeation chromatography, are generally used. However, such chromatographic purification needs lengthy and tedious steps, preventing the studies of lectins especially in case of small amount of target lectins in the starting materials. To overcome this problem, a simple and effective method is desired. Use of gold nano-particles having glycans is one of the most promising for the purpose.

Gold nano-particles having glycans were rapidly developed in this decade, and utilized to analyse lectins, to estimate their affinity strength or to visualize them with electron microscopy (*5–7*). Recently, we established an efficient technique for the immobilization of glycans on gold nano-particles (*8*, *9*). The produced gold nano-particles, designated sugar-immobilized gold nano-particles (SGNPs), were homogeneous in size and amount of glycans. Importantly, they are easily sedimented by forming aggregate with lectins, suggesting that they are promising for capturing lectins. In this study, we established an effective method for purification of lectins using the SGNPs. As a result, a lectin with high purity was successfully obtained from plant extract.

MATERIALS AND METHODS

Materials—All reagents were used without further purification. Banana was obtained from a grocery store and stored at −20°C until use. Sugars were purchased as follows: maltose, cellobiose and lactose were obtained from Nacalai tesque (Kyoto, Japan); GalNAcβ1-3Gal and α1-2 mannobiose from Dextra Lab. (Reading, UK); melibiose from TCI (Tokyo, Japan). GlcNAcα1-6Glc, GlcNAcβ1-6Glc, GalNAcα1-6Glc, Fucα1-6Glc, Fucβ1-6Glc were generous gifts from Dr Wakao (Kagoshima University).

*To whom correspondence should be addressed. Tel: +81-99-285-8369, Fax: +81-99-285-8369,
E-mail: ysuda@eng.kagoshima-u.ac.jp

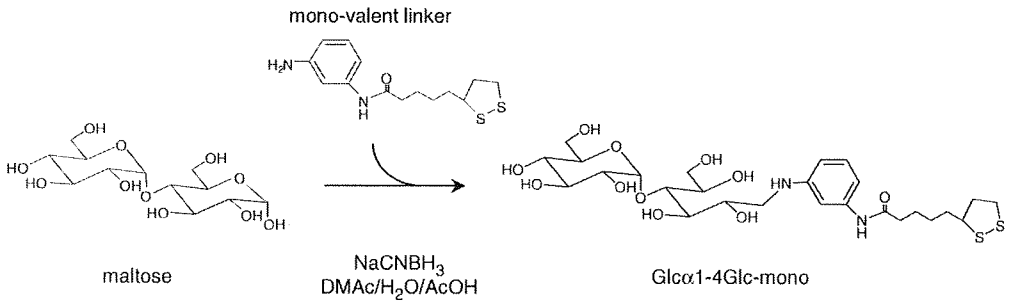

Fig. 1. Synthesis of ligand-conjugate containing α-D-glucoside (Glcα1-4Glc-mono).

Synthesis of Ligand-Conjugate Containing Sugar Moieties—Ligand-conjugates containing sugar-moieties were prepared according to the previous report (*8*, *9*). For preparation of ligand-conjugate containing α-D-glucoside (abbreviated as Glcα1-4Glc-mono), mono-valent linker compound (10.0 mg, 34 μmol) (*9*) dissolved in 1.0 ml of dimethylacetoamide (DMAc) was mixed with maltose (12.2 mg, 34 μmol, dissolved in 0.8 ml of distilled water) and 0.2 ml of acetic acid (Fig. 1). After incubation at 37°C for 4 h, $NaCNBH_3$ (21.3 mg, 340 μmol) dissolved in 0.2 ml of distilled water was added to the solution. After further incubation at 37°C for 72 h, the reaction was lyophilized. The obtained ligand-conjugate was purified by reverse-phase chromatography using Chromatorex ODS (Fuji Silysia Chemical, Aichi, Japan) equilibrated with 45% methanol at the flow rate of 0.8 ml/min. The obtained ligand conjugate was elucidated by reverse-phase chromatography using Inertsil ODS-3 (GL Science, Tokyo, Japan), MS (Voyager DE-Pro, Applied Biosystems, CA, USA) and ^1H NMR (ECA-600, JOEL, Tokyo, Japan).

By a similar protocol described above, the objected compound was prepared from appropriate materials, i.e. Glcβ1-4Glc-mono, Galα1-6Glc-mono, Galβ1-4Glc-mono, GlcNAcα1-6Glc-mono, GlcNAcβ1-6Glc-mono, GalNAcα1-6Glc-mono, GalNAcβ1-3Gal-mono, Fucα1-6Glc-mono, Fucβ1-6Glc-mono and Manα1-2Man-mono were prepared from cellobiose, melibiose, lactose, GlcNAcα1-6Glc, GlcNAcβ1-6Glc, GalNAcα1-6Glc, GalNAcβ1-3Gal, Fucα1-6Glc, Fucβ1-6Glc and α1-2 mannobiose, respectively.

Synthesis of SGNPs—Sugar-immobilized gold nanoparticles (SGNPs) were prepared according to the previous report (*8*). To synthesize α-D-glucoside immobilized SGNP (Glcα-GNP), 5 mM (final concentration) of $NaBH_4$ was added to 1 mM of aqueous solution of $NaAuCl_4$ with stirring. Above prepared 100 μM of ligand-conjugate (Glcα1-4Glc-mono) was then added to the solution with stirring. The resulting solution was subsequently dialysed against distilled water and PBST [100 mM phosphate buffer, pH 7.2, containing 0.9% (w/v) NaCl and 0.05% (v/v) Tween-20]. By TEM analysis, diameter of obtained particles was estimated to be 2–10 nm, and most of them showed around 5 nm.

Glcβ-GNP, Galα-GNP, Galβ-GNP, GlcNAcα-GNP, Glc NAcβ-GNP, GalNAcα-GNP, GalNAcβ-GNP, Fucα-GNP, Fucβ-GNP and Manα-GNP were prepared from appropriate ligand-conjugate, i.e. Glcβ1-4Glc-mono, Galα1-6Glc-mono, Galβ1-4Glc-mono, GlcNAcα1-6Glc-mono, GlcNAcβ1-6Glc-mono, GalNAcα1-6Glc-mono, GalNAcβ1-3Gal-mono, Fucα1-6Glc-mono, Fucβ1-6Glc-mono and Manα1-2Man-mono, with similar protocol. The SGNPs prepared were elucidated by binding experiment using lectins, e.g. Concanavalin A (Con A) purchased from EY Laboratories (CA, USA) and RCA120 from Vector Laboratories (CA, USA). The amount of sugar ligand attached to the gold nanoparticles was estimated by elemental analysis. As a result, 50–70 ligand-conjugates were immobilized on the surface of one gold nano-particle of 5 nm diameter.

Preparation of Plant Extract—Matured banana pulp (1 g) was homogenized in 5 ml of PBS [100 mM phosphate buffer, pH 7.2, containing 0.9% (w/v) NaCl] containing 10 mM 2-mercaptoethanol. The extract was stirred at 4°C for 2 h, and the homogenate was centrifuged at 8,000 r.p.m. for 30 min. Obtained supernatant was then filtered with DISMIC® ($\phi = 0.45$ μm, ADVANTEC, CA, USA). After adding 60% (w/v) ammonium sulphate to the filtrate, the precipitate was obtained by centrifugation at 10,000 r.p.m. for 10 min at 4°C. Thus, obtained precipitate was dissolved in 2.5 ml of PBS containing 10 mM 2-mercaptoethanol. This solution was used for the following purification steps of lectins.

Screening with SGNPs—To evaluate the sugar chain-binding properties of the extract from banana, a series of SGNPs, i.e. Glcα-GNP, Glcβ-GNP, Galα-GNP, Galβ-GNP, GlcNAcα-GNP, GlcNAcβ-GNP, GalNAcα-GNP, GalNAcβ-GNP, Fucα-GNP, Fucβ-GNP and Manα-GNP, was used for screening. In brief, the above 11 kinds of SGNP solution (30 μl, adjusted to $Abs_{530} = 3.0$) were mixed with 10 μl of sample solutions in round-bottomed microtitre plate wells, respectively, and incubated overnight at 4°C. Also, the extent of aggregation was determined by measuring the absorbance of supernatant at 530 nm. Activity was calculated according to the following equation:

$$\text{Precipitation (\%)} = 100 - \frac{Abs^{a}_{530}}{Abs^{b}_{530}} \times 100$$

where Abs^{b}_{530} and Abs^{a}_{530} indicate absorbance at 530 nm before and after overnight incubation, respectively.

Dissociation of SGNP–Lectin Complex with Free Sugars—Dissociation effects of free sugars against SGNP aggregates were examined. Similar to the screening described above, 30 μl of Glcα-GNP was mixed with

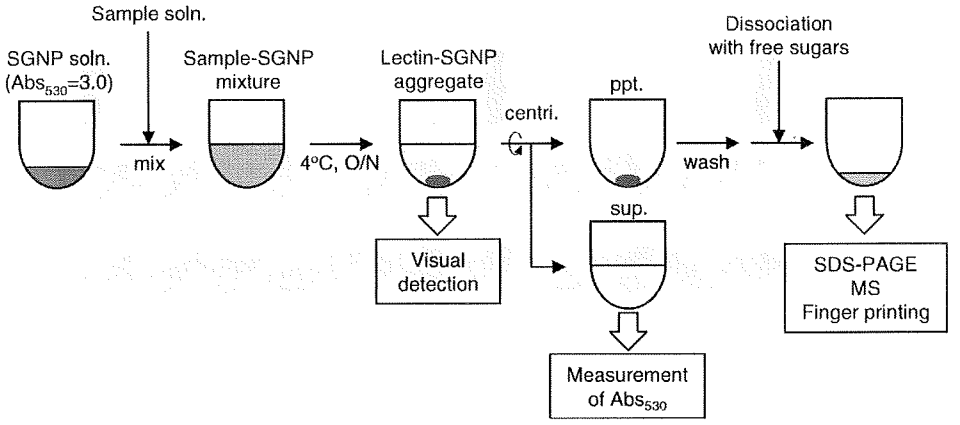

Scheme 1. **The procedure for capturing lectins using SGNPs.** Several SGNPs, e.g. Manα-GNP, Glcα-GNP and Galβ-GNP, can be used. After subsequent washing with appropriate buffer and distilled water, aggregate was dissolved in inhibitory sugar solutions and applied to subsequent analyses.

10 μl of sample solution. After standing at room temperature for 10 min, the formed SGNP aggregate was sedimented by centrifugation at 1,800 r.p.m. for 1 min at room temperature. After removal of supernatant, 100 μl of sugar solutions (0.2 M glucose, GlcNAc, mannose and galactose dissolved in distilled water) were added to each well.

Capturing Lectins—Sugar-binding proteins (lectins) were captured by SGNPs and characterized. The overall approach was shown in Scheme 1. From data of screening, 30 μl of Glcα-GNP, GlcNAcα-GNP or Manα-GNP was added to 10 μl of banana extract, and thoroughly mixed by pipetting. After incubation overnight at 4°C, the formed aggregate was sedimented by centrifugation at 10,500 r.p.m. for 10 min, and the supernatant was removed. After subsequent washing with 50 μl each of PBST and distilled water, the aggregate was dissolved by adding 10 μl of inhibitory monosaccharides, *i.e.* 0.2 M glucose, 0.2 M GlcNAc and 0.2 M mannose were used for Glcα-GNP, GlcNAcα-GNP and Manα-GNP, respectively. Thus, captured proteins were analysed by SDS–PAGE under non-reducing condition using 15% gel without further purification. Also, they were applied to the subsequent analyses described below.

Proteolytic Digestion by Trypsin—After re-dissolving in inhibitory sugar solutions, 10 μl aliquot of sample solution (corresponding to 2.3 μg protein) was added to the same volume of 75 mM NH_4HCO_3. Proteins in the solution were denatured by boiling for 5 min, and then 10 μl of trypsin (Sigma–Aldrich, MO, USA) dissolved in distilled water (5 μg/ml) was added. The protein digestion was performed by incubating the reaction solution at 37°C for 2 h. The resulting digest was analysed by MALDI-TOF/MS without further purification.

MALDI-TOF Mass Spectrometry—The MALDI-TOF mass spectrometer used was a Voyager DE-Pro (Applied Biosystems). α-cyano-4-hydroxycinnamic acid (CHCA) or 3,5-dimethyl-4-hydroxycinnamic acid (SA) as MALDI matrix was dissolved in the aqueous solution containing 50% acetonitrile and 0.1% trifluoroacetic acid (TFA) to make 10 mg/ml. SGNP-captured proteins and the trypsin-digested peptides were co-crystallized with CHCA or SA matrix. The MS analyses were performed with a reflector and positive-ion mode. The spectra were acquired with 300 shots of a 337 nm nitrogen laser operating at 3 Hz. Angiotensin (SIGMA) and Calibration mixture 2 (PE Biosystems, CA, USA) were used as MS calibration standards. Protein identification was performed by searching the National Center for Biotechnology Information (NCBI) non-redundant database using Mascot search engine (http://www.matrixscience.com/search_form_select.html). The following parameters were used for database searches with MALDI-TOF peptide mass fingerprinting: monoisotopic mass, ±1.2 Da peptide mass tolerance, trypsin as digestion enzyme with one missed cleavage allowed, no modification of a cysteine residue.

RESULTS AND DISCUSSION

To purify lectins from biological materials, the most efficient way may be to utilize their affinity for sugar chains. Since lectins specifically recognize sugar structures, it is essential to select appropriate sugar chains. Thus, we first screened the sugar-binding property of the extract using a series of SGNPs, i.e. Glcα-GNP, Glcβ-GNP, Galα-GNP, Galβ-GNP, GlcNAcα-GNP, GlcNAcβ-GNP, GalNAcα-GNP, GalNAcβ-GNP, Fucα-GNP, Fucβ-GNP and Manα-GNP. The banana extract was thoroughly mixed with 11 kinds of SGNPs and allowed to stand at 4°C. When banana extract includes agglutinin having affinity for particular SGNPs, lectin-SGNP aggregate may be formed, and it is visually detected as precipitate. As a result, three of the SGNPs tested, i.e. Glcα-GNP, GlcNAcα-GNP and Manα-GNP, obviously formed precipitate (Fig. 2). In contrast, no precipitate was detected for the other SGNPs including Glcβ-GNP and GlcNAcβ-GNP. To know the extent of aggregation, the absorbance of supernatant at 530 nm was measured. As shown in Fig. 2, 91.2%, 92.4% and 92.8% of Glcα-GNP, GlcNAcα-GNP and Manα-GNP, respectively, in the wells precipitated, while the β-anomers showed no or, if any, weak affinity for banana extract. These results clearly

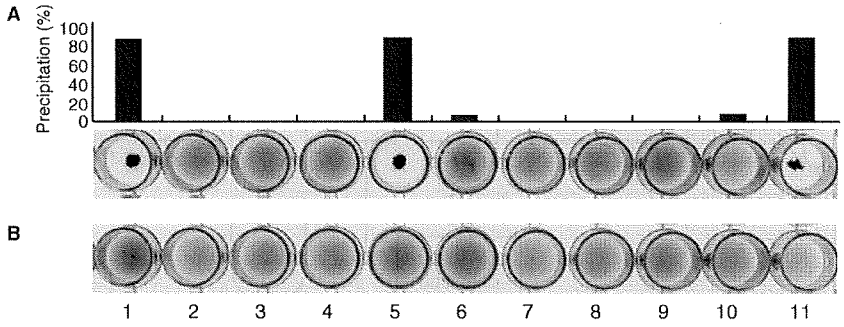

Fig. 2. **Screening of sugar-immobilized gold nano-particles (SGNPs).** Ten microlitres of sample solutions were added to 30 µl of each SGNP in round-bottomed microtitre plate wells. When the sample solution includes lectin(s) having affinity for particular SGNP(s), lectin–SGNP aggregate is formed and observed as a precipitate. Graphs indicate the extent of aggregation determined by measuring the absorbance of supernatant at 530 nm. (A) Banana extract, (B) PBST as negative control. 1: Glcα-GNP, 2: Glcβ-GNP, 3: Galα-GNP, 4: Galβ-GNP, 5: GlcNAcα-GNP, 6: GlcNAcβ-GNP, 7: GalNAcα-GNP, 8: GalNAcβ-GNP, 9: Fucα-GNP, 10: Fucβ-GNP, 11: Manα-GNP.

indicated that banana extract included agglutinin having affinity for α-glucose, α-GlcNAc and α-mannose. The sugar-binding specificity observed here agrees well with previous reports describing that lectin in banana pulp shows affinity for mannose, glucose, GlcNAc and their derivatives (*10–13*).

To clarify sugar-binding specificity in detail, dissociation effects of free sugars were examined using Glcα-GNP. Similar to the case of screening described above, 30 µl of Glcα-GNP was mixed with 10 µl of banana extract. After standing at room temperature for 10 min, aggregate was sedimented by centrifugation at 1,800 r.p.m. for 1 min, and supernatant was removed. To the wells, 100 µl of sugar solutions, i.e. 0.2 M glucose, 0.2 M GlcNAc, 0.2 M mannose or 0.2 M galactose dissolved in distilled water, was added, respectively. As expected, Glcα-GNP-aggregate was re-dissolved in glucose solution (Fig. 3). In addition, it was also re-dissolved in GlcNAc and mannose solution, but not at all in galactose solution (Fig. 3). The result indicated that the banana extract included an agglutinin having affinity for glucose, mannose and GlcNAc. In other words, the protein aggregated with Glcα-GNP, GlcNAcα-GNP or Manα-GNP may be identical.

Using Glcα-GNP, GlcNAcα-GNP or Manα-GNP, the purification of the agglutinin from banana extract was performed. As shown in Scheme 1, 10 µl of banana extract was added to 30 µl of each SGNP. The formed aggregates were sedimented by centrifugation, and supernatant was transferred to other tubes. Precipitates were subsequently washed with PBS containing 0.05% Tween-20 (PBST) and distilled water to remove non-specifically bound proteins and salt, and then re-dissolved in inhibitory sugar solutions. As estimated by quantifying the protein using a dye-binding assay (*14*), 2.3, 4.3 and 3.6 µg proteins were captured from 10 µl of extract (corresponding to 4 mg starting plant material) using Glcα-GNP, GlcNAcα-GNP and Manα-GNP, respectively. Higher yield relative to previous report (*11*) was probably achieved by one-tube reaction. Upon SDS–PAGE under non-reducing conditions, every SGNP-captured protein showed a single protein band at a molecular mass 13.6 kDa (Fig. 4, lanes 4, 6 and 8). No band was detected at the corresponding mass in

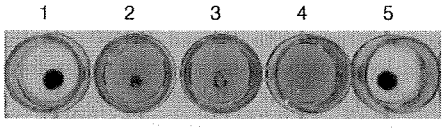

Fig. 3. **Dissociation of SGNP–lectin complex with free sugars.** Lectin–Glcα-GNP aggregate is first formed. After removal of supernatant, sugar solutions were added to each well. When lectin–SGNP interaction is inhibited by free sugars added, lectin will dissociate from the SGNP and the aggregate disappears. (1) PBS, (2) glucose, (3) GlcNAc, (4) mannose, (5) galactose.

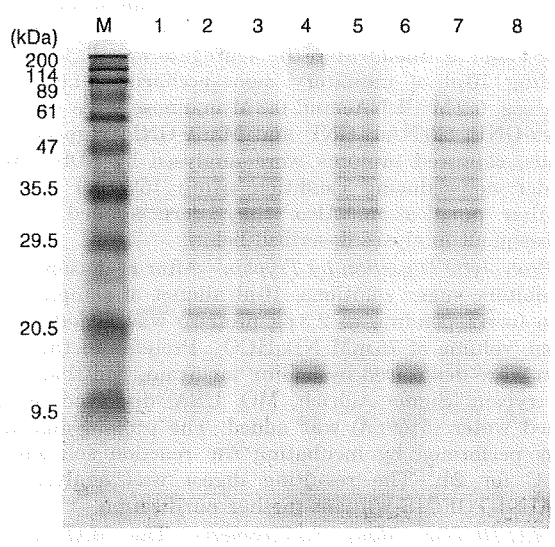

Fig. 4. **SDS–PAGE of proteins obtained from banana stained with CBB.** M: Molecular marker, lane 1: crude extract from plant materials, lane 2: extract after concentration with 60% (w/v) ammonium sulphate, lanes 3 and 4: Glcα-GNP, lanes 5 and 6: GlcNAcα-GNP, lanes 7 and 8: Manα-GNP. Lanes 3, 5 and 7: supernatant after aggregation, lanes 4, 6 and 8: precipitation after aggregation.

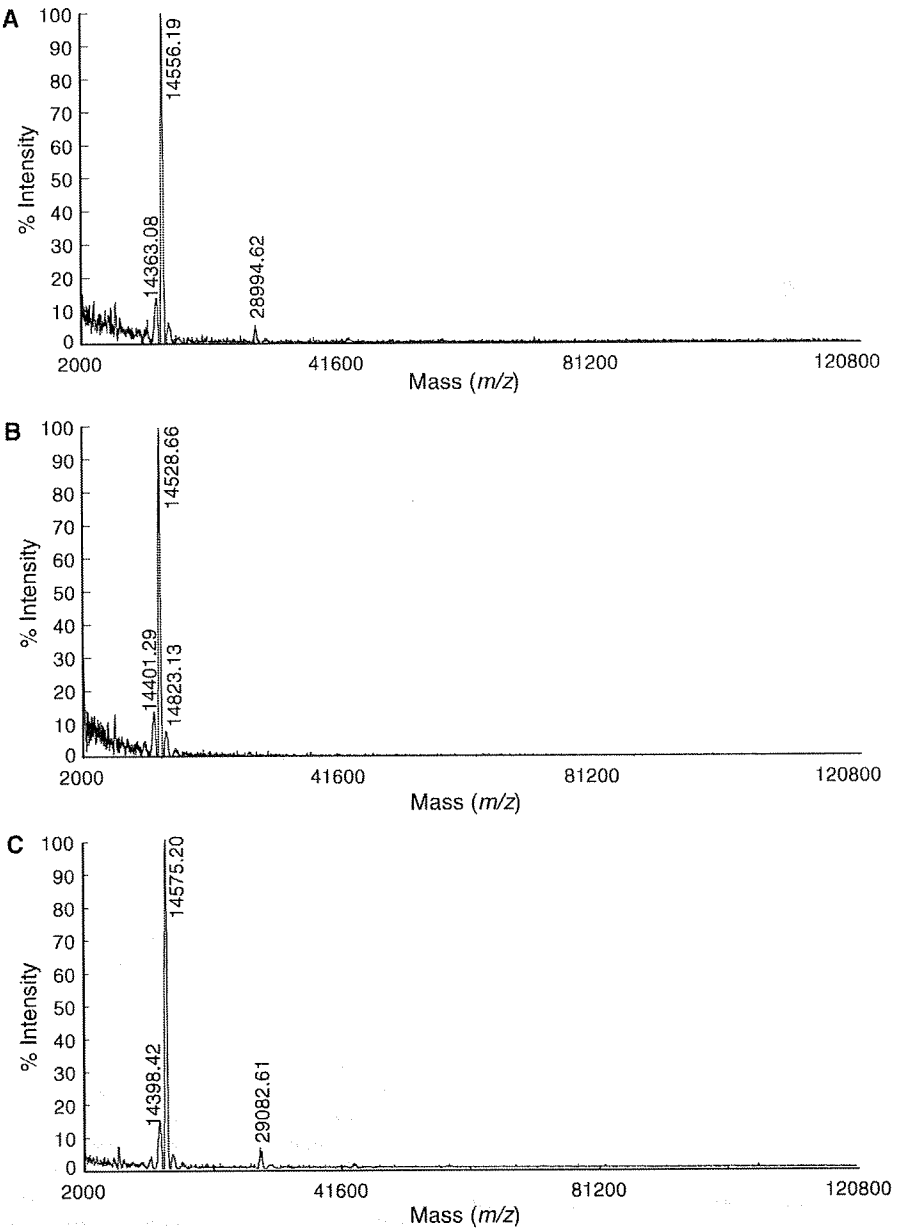

Fig. 5. **MALDI-TOF mass spectra of proteins obtained from banana extract using Glcα-GNP (A), GlcNAcα-GNP (B) and Manα-GNP (C).**

supernatant (Fig. 4, lanes 3, 5 and 7). This result indicated that the protein with molecular mass 13.6 kDa in the extract was completely captured by SGNPs. Also, the captured proteins are very pure, as far as stained with CBB.

Exact molecular mass of captured proteins was then measured By MALDI-TOF MS analysis. Since aggregates were washed with distilled water and dissolved in sugar solutions without salts, SGNP-captured proteins were used for MS analysis without further purification and desalting steps. For analysis, 1.2, 2.2 and 1.8 μg of Glcα-GNP-, GlcNAcα-GNP- and Manα-GNP-captured proteins (corresponding to 5 μl of extract, *i.e.* 2 mg of starting plant material), respectively, was co-crystallized with SA, and directly analysed by MALDI-TOF mass spectrometer. As a result, intense signals were detected for all the three samples (Fig. 5), in spite of remaining free SGNPs. The result indicates that free SGNPs did not disturb the ionization of proteins in MALDI-TOF/MS, suggesting that the SGNP was not needed to be removed from the analytical samples. In case of Glcα-GNP-captured protein, only one major peak was detected at *m/z* value of 14,556 (Fig. 5A). According to the previous report, mannose/glucose-binding lectin from banana pulp

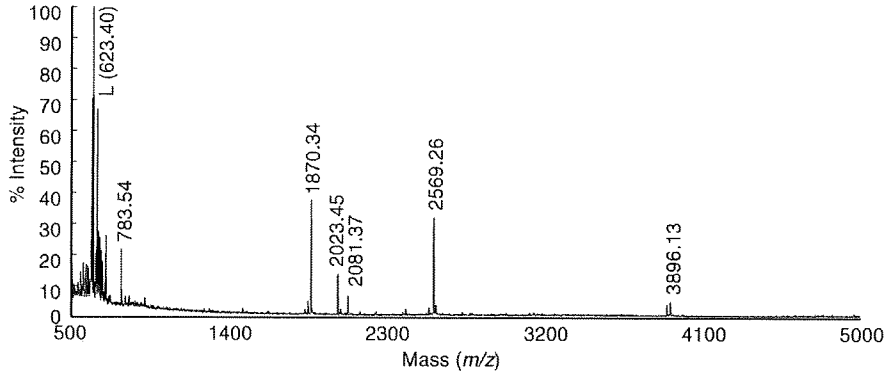

Fig. 6. **MALDI-TOF mass spectra from tryptic digestion of proteins obtained from banana extract using Glcα-GNP.** All the six peaks submitted to the Mascot search engine for database searching was matched for total sequence coverage of 76%. L denotes *m/z* value of ligand conjugate.

Table 1. **Peptide peaks detected from the tryptic digestion of Glcα-GNP-captured proteins.**

	m/z	Protein	Start–End	Missed cleavage	Sequence
1	1870.40	Banana lectin	7–25	0	VGAWGGNGGSAFDMGPAYR
2	2081.37	Banana lectin	31–49	0	IFSGDVVDGVDVTFTYYGK
3	2569.26	Banana lectin	31–53	1	IFSGDVVDGVDVTFTYYGKTETR
4	3896.13	Banana lectin	54–91	0	HYGGSGGTPHEIVLQEGEYLVGMAGEVANYHGAVVLGK
5	2023.45	Banana lectin	100–120	0	AYGPFGNTGGTPFSLPIAAGK
6	783.55	Banana lectin	121–127	0	ISGFFGR

is a dimeric protein composed of 15 kDa subunits estimated by SDS–PAGE (*10*, *11*). In addition, its molecular weight calculated from sequence (Accession No: 2BMYA) is 14,554 Da (*15*). Thus, the captured protein is supposed to be a banana lectin. Since gene of banana lectin is a member of a multi-gene family (*11*), a weak signal at *m/z* value of 14,363 might be derived from them. Another minor signal at *m/z* value of 28,994 was corresponding to a dimer of banana lectin. Very similar MS profiles were observed for GlcNAcα-GNP and Manα-GNP (Fig. 5B and C). In both cases, only one major peak was detected around m/z = 14,550. The *m/z* value of major peaks observed for GlcNAcα-GNP and Manα-GNP were 14,528 and 14,575, respectively, which are corresponding to the previous report, too (*11*). According to the results of MS analysis together with those of SDS–PAGE, the purity of captured proteins was high enough to apply further analysis.

To identify SGNP-captured protein, we carried out peptide-mass fingerprinting. Judging from the results of dissociation of SGNP–lectin complex with free sugars, SDS–PAGE and MS spectrometry described above (Figs 3, 4 and 5), all the proteins captured by Glcα-GNP, GlcNAcα-GNP and Manα-GNP were supposed to be identical. Thus, Glcα-GNP-captured protein was used for the purpose. As described under MATERIALS AND METHODS section, the captured protein (2.3 μg protein) was digested by trypsin, and the resulting digests were analysed by the MALDI-TOF/MS (Fig. 6). Detected peaks at *m/z* 783.54, 1870.34, 2023.45, 2081.37, 2569.26 and 3896.13 were searched against the Swiss-Prot protein database for the identification of source proteins. All six peaks matched the database. The peptide sequences from the digested protein are listed in Table 1. As expected, all the peaks are revealed to be derived from banana lectin. The sequence coverage was 76%. Thus, Glcα-GNP-captured protein was identified as banana lectin. This result indicated that the purity of protein captured by Glcα-GNP was sufficient to identify the source protein.

In conclusion, we established an effective method for a one-step purification of lectin from extracts using SGNPs. Compared with conventional methods, several advantages of SGNPs were found, e.g. small amount of start materials (in case of banana lectin, <1 g), simple operation (only centrifugation) and direct analysis by SDS–PAGE and MS spectrometry (without further purification or concentration steps). Although SGNPs having simple saccharides were used here, a lectin was successfully purified with such high purity as to identify the source protein. Using a similar protocol, we have also performed easy and quick purification of lectins from soybean. Since, in general, affinities of lectins for oligosaccharides are relatively high compared with those for simple saccharides, utilization of SGNPs having complex glycans is promising for easy purification of less abundant carbohydrate-binding proteins.

We thank Y. Fujimoto, Osaka University, for her help in elemental analysis. This research was supported in part by a grant from a Ministry of Health, Labor and Welfare (Y.S.), and Japan Science and Technological Agency (CREST, Y.S.).

REFERENCES

1. Sharon, N. and Lis, H. (2003) *Lectins*. 2nd edn, pp. 1–4 Kluwer Academic Publishers, Boston

2. Kijune, J.W. (1996) Function of plant lectins. *Chemtracts – Biochem. Mol. Biol.* **6**, 180–187
3. Van Damme, E.J.M., Peumans, W.J., Pusztai, A., and Bardocz, S. (1998) *Handbook of Plant Lectins: Properties and Biomedical Applications*. p. 452 John Wiley and Sons, Chichester
4. Murdock, L.L. and Shade, R.E. (2002) Lectins and protease inhibitors as plant defenses against insects. *J. Agric. Food. Chem.* **50**, 6605–6611
5. Otsuka, H., Akiyama, Y., Nagasaki, Y., and Kataoka, K. (2001) Quantitative and reversible lectin-induced association of gold nanoparticles modified with alpha-lactosyl-omega-mercapto-poly(ethylene glycol). *J. Am. Chem. Soc.* **123**, 8226–8230
6. Hone, D.C., Haines, A.H., and Russell, D.A. (2003) Rapid, quantitative calorimetris detection of a lectin using mannose-stabilized gold nanoparticles. *Langmuir* **19**, 7141–7144
7. Lin, C.C., Ye, Y.C., Yang, C.Y., Chen, C.L., Chen, G.F., Chen, C.C., and Wu, Y.C. (2002) Selective binding of mannose-encapsulated gold nanoparticles to type 1 pili in Escherichia coli. *J. Am. Chem. Soc.* **124**, 3508–3509
8. Suda, Y., Kishimoto, Y., Nishimura, T., Yamashita, S., Hamamatsu, M., Saito, A., Sato, M., and Wakao, M. (2006) Sugar-immobilized gold nano-particles (SGNP): novel bioprobe for the on-site analysis of the oligosaccharide protein interactions. *Polymer Preprints* **47**, 156–157
9. Suda, Y., Arano, A., Fukui, Y., Koshida, S., Wakao, M., Nishimura, T., Kusumoto, S., and Sobel, M. (2006) Immobilization and clustering of structurally defined oligosaccharides for sugar chips: an improved method for surface plasmon resonance analysis of protein carbohydrate interactions. *Bioconjug. Chem.* **17**, 1125–1135
10. Koshte, V.L., van Dijk, W., van der Stelt, M.E., and Aalberse, R.C. (1990) Isolation and characterization of BanLec-I, a mannoside-binding lectin from *Musa paradisiac* (banana). *Biochem. J.* **272**, 721–726
11. Peumans, W.J., Zhang, W., Barre, A., Houles Astoul, C., Balint-Kurti, P.J., Rovira, P., Rouge, P., May, G.D., Van Leuven, F., Truffa-Bachi, P., and Van Damme, E.J.M. (2000) Fruit-specific lectins from banana and plantain. *Planta* **211**, 546–554
12. Mo, H., Winter, H.C., Van Damme, E.J., Peumans, W.J., Misaki, A., and Goldstein, I.J. (2001) Carbohydrate binding properties of banana (*Musa acuminata*) lectin I. Novel recognition of internal alpha1,3-linked glucosyl residues. *Eur. J. Biochem.* **268**, 2609–2615
13. Winter, H.C., Oscarson, S., Slattegard, R., Tian, M., and Goldstein, I.J. (2005) Banana lectin is unique in its recognition of the reducing unit of 3-O-beta-glucosyl/mannosyl disaccharides: a calorimetric study. *Glycobiology* **15**, 1043–1050
14. Bradford, M. (1976) A rapid and sensitive method for the quantitation of microgram quantities of protein utilizing the principle of protein-dye binding. *Anal. Biochem.* **72**, 248–254
15. Meagher, J.L., Winter, H.C., Ezell, P., Goldstein, I.J., and Stuckey, J.A. (2005) Crystal structure of banana lectin reveals a novel second sugar binding site. *Glycobiology* **15**, 1033–1042

Bulletin of the Chemical Society of Japan

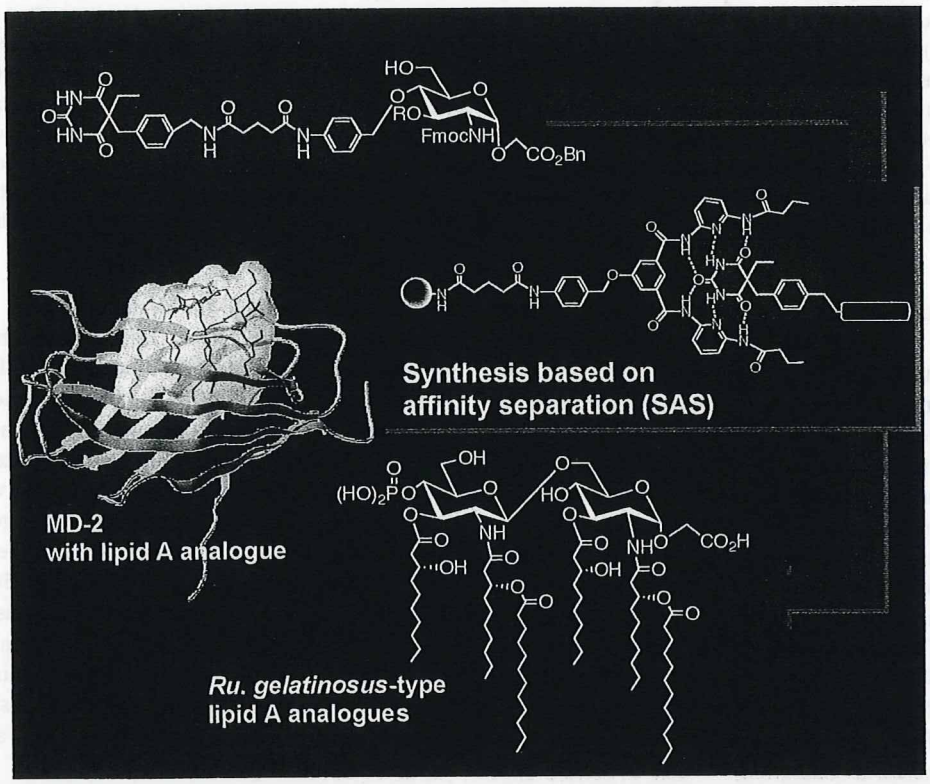

BCSJ Award Article by Yukari Fujimoto et al.

Vol. 81, No. 7

July 15
2008

BCSJ Award Article

Synthesis of *Rubrivivax gelatinosus* Lipid A and Analogues for Investigation of the Structural Basis for Immunostimulating and Inhibitory Activities

Yoshiyuki Fukase,[1] Yukari Fujimoto,*[1] Yo Adachi,[1] Yasuo Suda,[2] Shoichi Kusumoto,[1,3] and Koichi Fukase*[1]

[1]Department of Chemistry, Graduate School of Science, Osaka University, 1-1 Machikaneyama Toyonaka, Osaka 560-0043

[2]Department of Nanostructure and Advanced Materials, Graduate School of Science and Engineering, Kagoshima University, Kagoshima 890-0065

[3]Suntory Institute for Bioorganic Research, Shimamoto-cho, Mishima-gun, Osaka 618-8503

Received December 3, 2007; E-mail: yukarif@chem.sci.osaka-u.ac.jp

To elucidate the structural requirements for the endotoxic and antagonistic activities of lipid A derivatives, we have focused on the effects of the acyl moieties and acidic groups at the 1- and 4′-positions in the present study. We have synthesized new analogues corresponding to *Rubrivivax gelatinosus* lipid A, which has a characteristic symmetrical distribution of its acyl groups on its two glucosamine residues with shorter acyl groups (decanoyl groups (C_{10}) and lauryl groups (C_{12})) than *Escherichia coli* lipid A's. Carboxymethyl (CM) analogues in which one of the phosphates was replaced with a CM group were also synthesized with a different distribution of acyl groups. Biological tests revealed that the acyl group distribution in the lipid A analogue, strongly affected its bioactivity. The synthetic *Ru. gelatinosus* type lipid A showed potent antagonistic activity against LPS, whereas its 1-*O*-carboxymethyl analogue showed weak endotoxic activity. These results demonstrate that when lipid A has shorter (C_{10} and C_{12}) hexa-acyl groups, its bioactivity is more easily affected by small structural differences, such as differences in acidic groups or acyl group distribution, and that they can change bioactivity from endotoxic to agonistic or vice versa at this structural boundary for the bioactivity.

The innate immune system is a phylogenetically ancient defense mechanism conserved between plants and animals.[1–5] One of the important roles of innate immunity is the detection of invading pathogens (bacteria, fungi, viruses, etc.) through innate immune receptors that recognize characteristic structures that are present in microorganisms, called PAMPs (pathogen-associated molecular patterns). PAMPs are essential molecules for pathogens that are not found within the host. In vertebrates, two diverse families of receptors, i.e., the Toll-like receptor (TLR) and Nod-like receptor (NLR) families, detect PAMPs such as the bacterial cell wall peptidoglycan (PGN), lipopolysaccharide (LPS) of Gram-negative bacteria, lipoproteins, bacterial DNA, viral RNA, etc. to activate the immune system. Most PAMPs therefore show immunostimulating activity.

LPS is a cell surface glycoconjugate of Gram-negative bacteria that is also known as endotoxin,[6–12] and is sensed by a receptor complex consisting of TLR4 and its adaptor protein MD-2. Via this complex, LPS stimulates immunocompetent cells such as macrophages and monocytes to produce a variety of mediators, e.g., cytokines, prostaglandins, the platelet activating factor, oxygen free radicals, and NO. These mediators activate and modulate the immune system. If too much LPS is released during a severe Gram-negative bacterial infection, the overproduction of these mediators can lead to endotoxin-related symptoms such as high fever, serious inflammation, hypotension, and, in serious cases, lethal shock.

LPS consists of a glycolipid component termed lipid A that is covalently bound to a polysaccharide. It was unequivocally proved that lipid A is the chemical entity responsible for the biological activity of LPS by the total synthesis of *Escherichia coli* lipid A **1** (synthetic **1** is termed 506) (Figure 1) in 1984.[13,14] Lipid A specimens from various bacterial origins were shown to be closely related structurally and to consist of: 1) $\beta(1\rightarrow6)$ disaccharide of D-glucosamines, 2) phosphono groups at their reducing ends and the 4-position of their non-reducing glucosamines, and 3) long-chain acyl groups bound at 2, 2′, 3, and 3′ positions.

The recognition of LPS and lipid A by the TLR4/MD-2 receptor complex has been of major interest in the endotoxin research field.[1–12] To further our understanding of this issue, we investigated the precise structural requirements for lipid A biological activity. It has been previously shown that the acidic

Published on the web July 10, 2008; doi:10.1246/bcsj.81.796

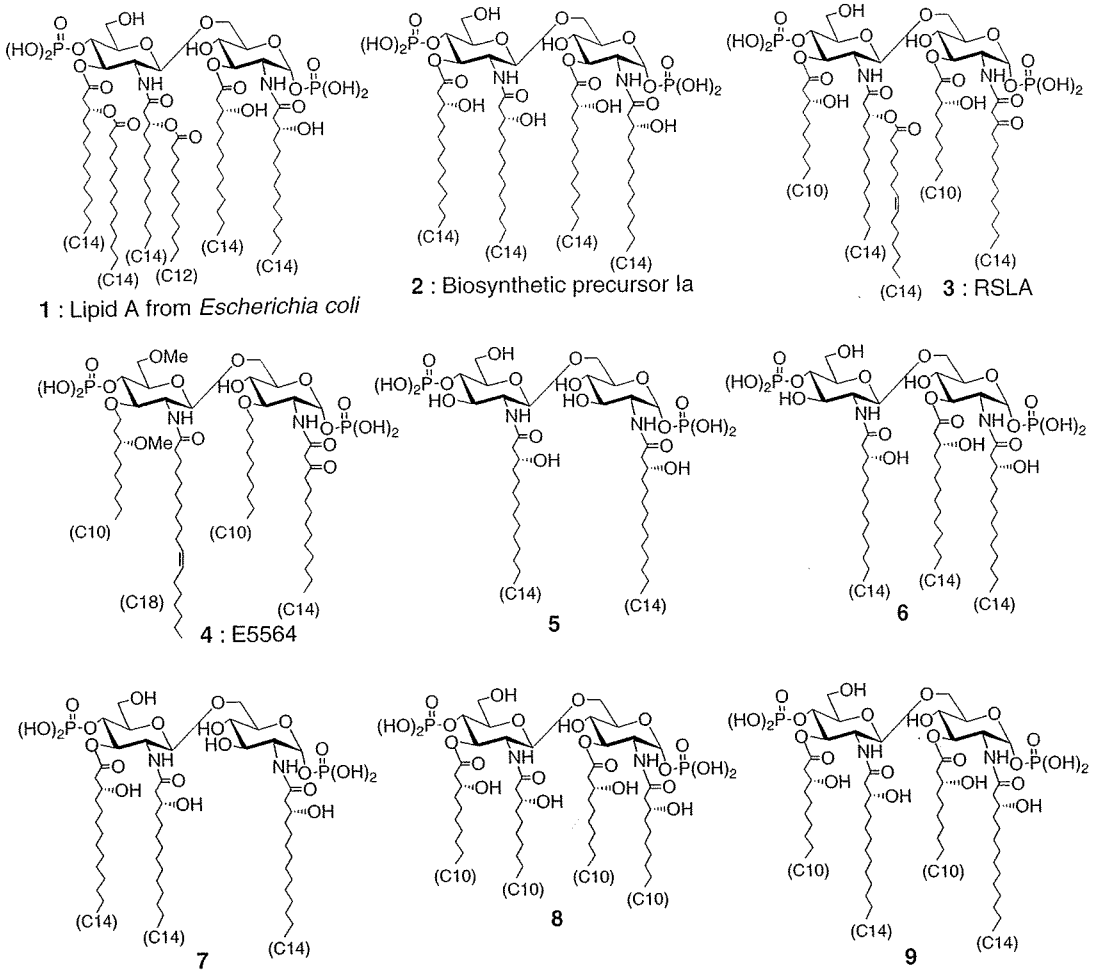

Figure 1. Structures of lipid A and its analogues with various acyl groups.

functional groups and acyl groups of lipid A are crucial for its biological activity.[15–18] Additionally, its phosphate groups can be replaced by other acidic groups (such as carboxylic acid) without decisively influencing its biological activity.[19–21] In contrast, the structure, number, and chain length of the acyl groups can dramatically influence its biological activity. The tetraacyl biosynthetic precursor of lipid A **2** (synthetic **2** is termed 406) has weaker but clear endotoxic activity in mice, but quite interestingly it also acts as an antagonist to LPS and lipid A **1** in human systems.[16,17] *Rhodobacter sphaeroides* lipid A **3** (RSLA) also shows species-related antagonistic or agonistic activities in different mammalian hosts.[22] The synthetic compounds E5531 and E5564 (Eritoran) **4** exhibit potent antagonistic activity in human systems.[23,24] RSLA, E5531, and E5564 each have acyl groups containing unsaturated and 2-keto acyl groups. E5564 is currently under development as a possible clinical therapeutic for the treatment of sepsis and septic shock. The *N,N'*-diacyl analogue **5** does not show any activity, but the triacyl-type analogues **6** and **7**, which lack acyl groups at the 3- and 3'-O-positions, show a weak but definite ability to inhibit the induction of IL-6 by LPS. Precursor-type analogues with shorter acyl chains have also been synthesized.[25] Analogue **9**, which possesses two (*R*)-3-hydroxytetradecanoic acids at the 2- and 2'-N-positions and two (*R*)-3-hydroxydecanoic acids at the 3- and 3'-O-positions, shows definite but ca. 10–100 times less potent antagonistic activity than natural-type **2**; whereas analogue **8**, which possesses four (*R*)-3-hydroxydecanoic acids, does not show this activity. On the other hand, Boons et al. revealed that an *E. coli* lipid A analogue had shorter lipids (two C14 and four C12 acids) that were ca. 100 times more active than *E. coli* lipid A.[26] They also synthesized heptaacylated *Salmonella typhimurium* lipid A, which showed much weaker activity than *E. coli* lipid A, and using its short-chain analogue they obtained similar results.

In this study, we focused on the structural requirements for the endotoxic and antagonistic activities of lipid A derivatives, and in particular, their effects on the human innate immune system. We particularly considered the effects of the acyl and acidic groups, and thus prepared and analyzed various structural analogues, including some with different numbers and distributions of acyl moieties on the lipid A backbone and some with a carboxymethyl group instead of a phosphate group.

Rubrivivax gelatinosus-type lipid A **10a** and **10b** (Figure 2) has shorter acyl groups than *E. coli* lipid A **1**, and a symmetrical (3 + 3) acylation distribution. It was reported that natural lipid A isolated from *Ru. gelatinosus* showed endotoxic activity.[27] By contrast, *Chromobacterium violaceum* lipid A **11** has acyl groups that are similar to *Ru. gelatinosus* and shows antagonistic activity.[28] The only structural difference between **10** and **11** is the chain lengths of three acyl groups. Since

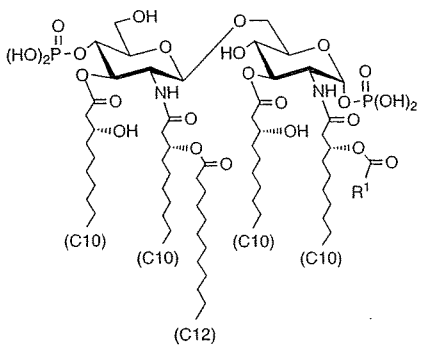

Lipid A from *Rubrivivax gelatinosus*
10a : $R^1CO = C_{11}H_{23}CO$ (C12)
10b : $R^1CO = C_{13}H_{27}CO$ (C14)

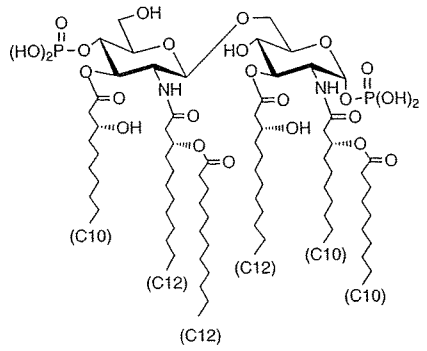

11 : Lipid A from *Chromobacterium violaceum*

Figure 2. Structures of two natural lipid A molecules that each have six acyl groups with symmetrical distributions.

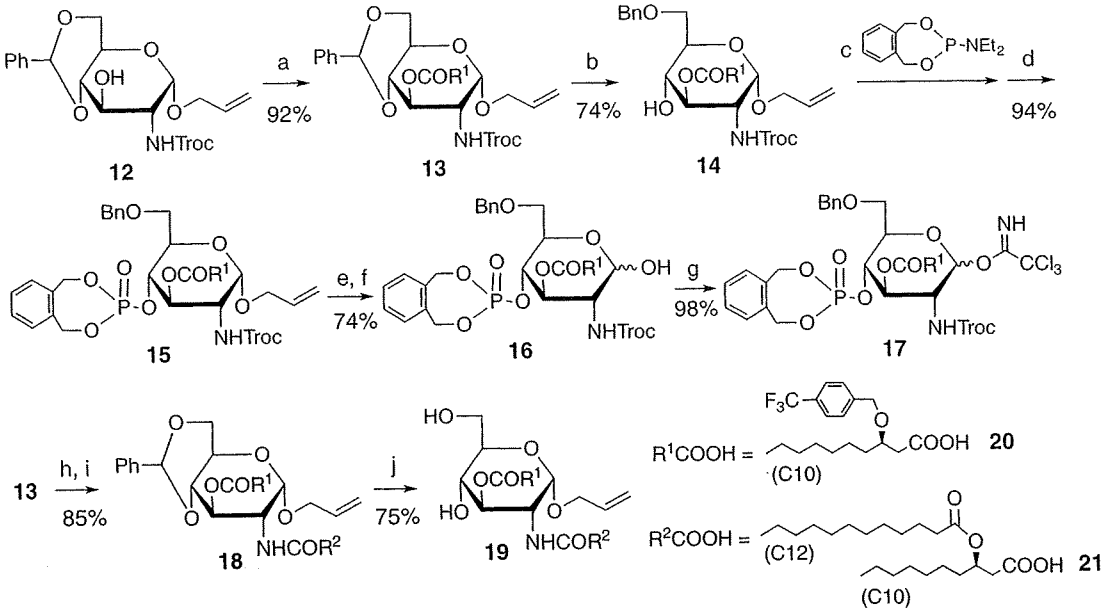

Scheme 1. Reagents and conditions: (a) R^1COOH (**20**), DCC, DMAP, CH_2Cl_2, rt, 17 h; (b) $BF_3 \cdot Et_2O$, Et_3SiH, CH_3CN, 0 °C, 1.5 h; (c) 1*H*-tetrazole, CH_2Cl_2, rt, 50 min; (d) *m*CPBA, −20 °C, 20 min; (e) $[Ir(cod)(MePh_2P)_2]PF_6$, H_2, THF, 2 h; (f) I_2, H_2O, rt, 30 min; (g) CCl_3CN, Cs_2CO_3, CH_2Cl_2, rt, 2 h; (h) Zn–Cu couple, AcOH, rt, 3 h; (i) R^2COOH (**21**), DCC, CH_2Cl_2, rt, 2 h; (j) TFA, H_2O, CH_2Cl_2, 0 °C, 2.5 h.

we were interested in the structural requirement for the endotoxic/antagonistic activity of lipid A with symmetrical (3 + 3) acylation distribution, *Ru. gelatinosus* lipid A **10a** was synthesized and analyzed in the present study.

Results

The Synthesis and Biological Activity of *Ru. gelatinosus* Lipid A. We have established the efficient synthesis of lipid A and analogues in our previous studies.[20,21,25,29] In the present study, *Ru. gelatinosus* lipid A **10a** was synthesized using a similar strategy (Scheme 1). The hydroxy and phosphate groups were protected with benzyl-type protective groups, which were removed by catalytic hydrogenation in the last step. The $\beta(1\rightarrow6)$ disaccharide structures were constructed by glycosylation of the glycosyl acceptor **19** with the *N*-Troc trichloroacetimidate donor **17** (Troc = 2,2,2-trichloroethoxycarbonyl). A Lewis acid catalyzed activation was used for the glycosylation with the trichloroacetimidate **17**.[30]

The glycosyl donor **17** and the glycosyl acceptor **19** were synthesized as shown in Scheme 1. The hydroxy group at the 3-position of 1-*O*-allyl 4,6-*O*-benzylidene-2-deoxy-2-(2,2,2-trichloroethoxycarbonylamino)-α-D-glucopyranoside[20] (**12**) was acylated with (*R*)-3-(4-trifluoromethylbenzyloxy)-decanoic acid (**20**). An unsubstituted benzyl group used for protecting the hydroxy function on the 3-hydroxyacyl residue proved to be prone to air-oxidation and gradually transformed into a corresponding benzoyl group. The *p*-trifluoromethylbenzyl group at this position was resistant to oxidation, but was readily removable by conventional hydrogenolysis.[21,30–33] Regioselective reductive opening of the benzylidene of **13** with $BF_3 \cdot OEt_2$ and Et_3SiH gave the 6-*O*-benzyl-4-OH GlcN derivative **14**.[34]

The free 4-hydroxy group of **14** was treated with Watanabe's reagent and 1-*H*-tetrazole, and then with *m*-chlo-

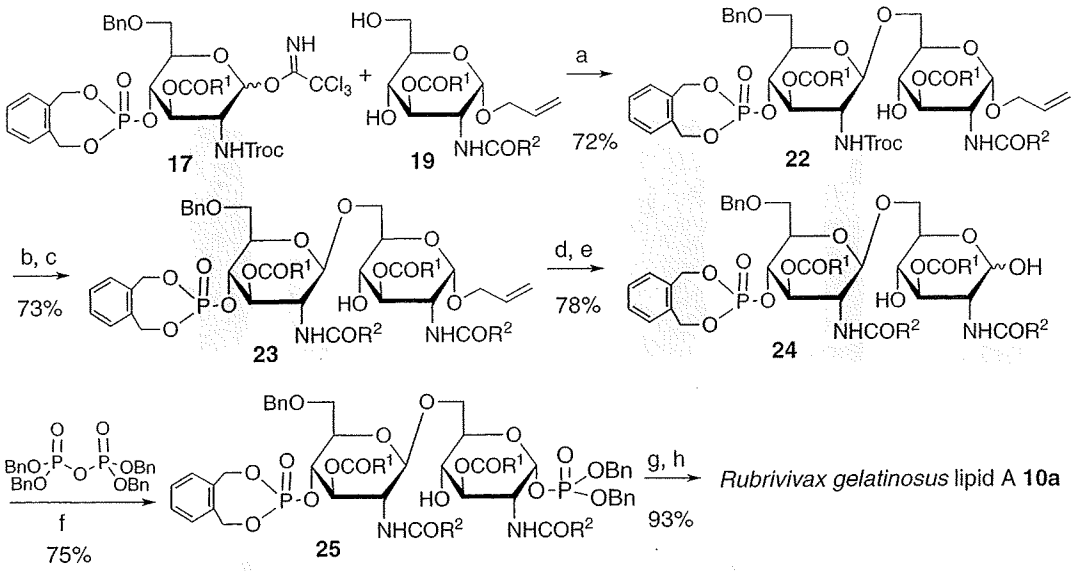

Scheme 2. Reagents and conditions: (a) TMSOTf, CH_2Cl_2, MS4A, −20 °C, 1 h; (b) Zn, AcOH, rt, 1.5 h; (c) R^2COOH (**21**), WSCD·HCl, HOBt, CH_2Cl_2, rt, 21 h; (d) $[Ir(cod)(MePh_2P)_2]PF_6$, H_2, THF, rt, 2 h; (e) I_2, H_2O, rt, 1 h; (f) $LiN(TMS)_2$, THF, −78 °C, 1.5 h; (g) H_2 (20 kg cm^{-2}), Pd-black, THF, rt, 44 h; (h) liquid–liquid partition column chromatography using Sephadex LH-20, $CHCl_3$–MeOH–H_2O–*i*PrOH (8:8:6:1).

roperbenzoic acid (*m*CPBA) to furnish the phosphate **15** in 94% yield.[35] The 1-*O*-allyl group of **15** was removed via isomerization to a 1-propenyl group and subsequently treated with iodine.[36] The resulting 1-OH sugar **16** was then transformed into the glycosyl trichloroacetimidate **17** by treatment with CCl_3CN and Cs_2CO_3.[37]

The glycosyl acceptor **19** was synthesized as follows. The 2-*N*-Troc group of **13** was removed using Zn–Cu and acetic acid and the resulting 2-amino group was then acylated with (*R*)-3-(dodecanoyloxy)decanoic acid (**21**) to give the 2,3-diacyl derivative **18**. Deprotection of the benzylidene group of **18** under the acidic conditions gave the glycosyl acceptor **19**.

Glycosylation of the above glycosyl acceptor **19** with the glycosyl donor **17** gave the desired $\beta(1\rightarrow6)$ disaccharide **22** in 72% yield (Scheme 2). The 2′-*N*-Troc group of **22** was cleaved and the resulting amino group was acylated with (*R*)-3-(dodecanoyloxy)decanoic acid (**21**) to give the fully acylated compound **23**. The allyl group at the 1-position of **23** was cleaved via isomerization to a vinyl group with an iridium complex to give **24** in 78% yield. After selective phosphorylation at the anomeric position with tetrabenzyl pyrophosphate, all the benzyl-type protecting groups in **25** were removed by catalytic hydrogenolysis to give the desired *Ru. gelatinosus* lipid A **10a**.

The biological activities of **10a** were evaluated in comparison to the corresponding LPS (*E. coli* O111:B4) by measuring typical endotoxic activity such as *Limulus* activity and cytokine induction. Cytokine inducing activity was tested in human peripheral whole-blood cells.[38] A mixture of a test sample and heparinized human peripheral whole-blood collected from an adult volunteer in RPMI 1640 medium (Flow Laboratories, Irvine, Scotland) was incubated at 37 °C in 5% CO_2 for 24 h. The levels of cytokines, i.e., interleukin-6 (IL-6) and tumor necrosis factor-α (TNF-α), in supernatants of incubated mixtures were measured using an enzyme-linked immunosorbent assay (ELISA). Antagonistic activity was examined and compared to the tetraacyl biosynthetic precursor of lipid A (compound 406) **2** using an assay that measured the ability of a compound to inhibit LPS-induced cytokine production as follows. Samples, LPS (10 ng mL^{-1}) (*E. coli* O111:B4; Sigma Chemicals Co.), and heparinized human peripheral whole blood were mixed and incubated, and the levels of IL-6 and TNF-α were measured (as described above).

Table 1. The *Limulus* Activity of **10a**, **26a–26f**, and LPS (*E. coli* 0111:B4), as Tested Using an Endospecy Test® (Seikagaku Corporation, Tokyo)

	ED50/pg mL^{-1}
Ru. gelatinosus lipid A (**10a**)	10
CM analogue **26a**	5000
26b	10000<
26c	—
26d	10000<
26e	50
26f	50
LPS (*E. coli* 0111:B4)	50

The *Limulus* activity, the hemolymph coagulation activity on horseshoe crab amoebocyte lysates, was evaluated by the activation of factor *C* at various concentrations using an Endospecy Test® (Seikagaku Corporation, Tokyo) with *E. coli* O111:B4 LPS as a positive standard. As clearly seen in Table 1, *Ru. gelatinosus* lipid A **10a** showed potent *Limulus* activity that was comparable to *E. coli* LPS.

Ru. gelatinosus lipid A **10a** showed no cytokine inducing activity, but a potent ability to antagonize LPS endotoxic activity that was comparable to 406 (**2**) (Figure 3). As mentioned above, natural *Ru. gelatinosus* lipid A has immunostimulatory activity. In contrast, *Chromobacterium violaceum* lipid A **11**, which has acyl groups similar to *Ru. gelatinosus*, showed antagonistic activity. Both of these lipid A molecules have shorter acyl groups than *E. coli* lipid A, and symmetric (3 + 3) acylation distribution. Therefore, our study indicated that these

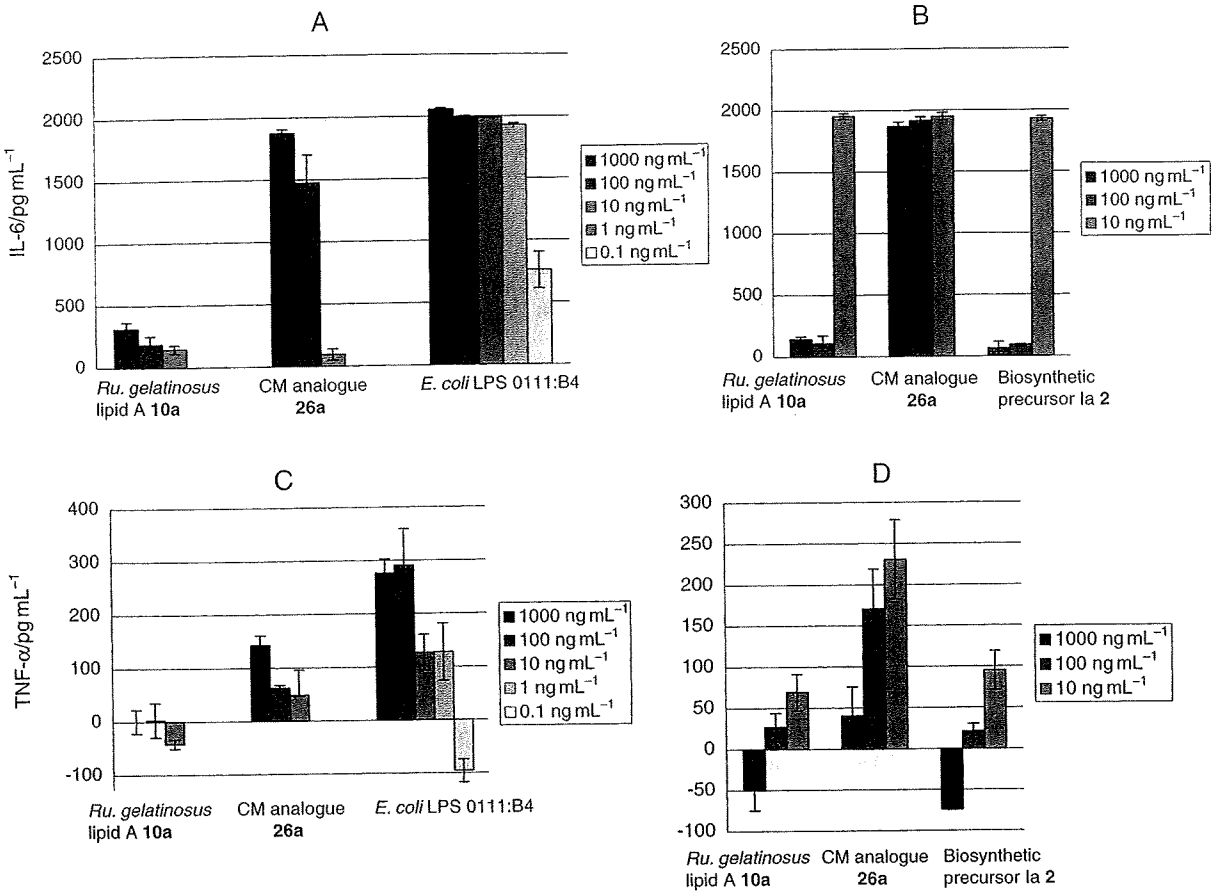

Figure 3. Cytokine inducing activity and inhibitory activity of *Ru. gelatinosus* lipid A **10a**, its CM analogue **26a**, and *E. coli* LPS 0111:B4 in human peripheral whole-blood cells. A: IL-6 inducing activity, B: inhibitory activity against IL-6 induction by *E. coli* LPS 0111:B4 (10 ng mL^{-1}), C: TNF-α inducing activity, D: Inhibitory activity against TNF-α induction by *E. coli* LPS 0111:B4 (10 ng mL^{-1}).

types of lipid A should show antagonistic activity. The reason why natural *Ru. gelatinosus* lipid A showed immunostimulatory activity will be discussed later.

Synthesis of *Ru. gelatinosus* Lipid A Analogues by Using Affinity Separation Method. We were then interested in the effect of acylation distribution on endotoxic/antagonistic activity and planned to synthesize six kinds of *Ru. gelatinosus* lipid A analogues **26a–26f** having hexaacyl groups (Figure 4). All of these compounds contained the same acyl groups but their distributions were different: each compound has two (*R*)-3-hydroxydecanoyl groups and two (*R*)-3-(dodecanoyloxy)decanoyl groups. Analogue **26c** had the same acylation pattern as *E. coli* lipid A **1**, so it was expected that biological tests of **26c** would give additional information on how chain length effected bioactivity.

1-*O*-Carboxymethyl (CM) analogues, which had glycosyl CM groups instead of the glycosyl phosphate moiety in natural lipid A, were chosen as targets, since they were easier to synthesize than the natural-type because of the chemical instability of the glycosyl phosphate. We previously synthesized both the *E. coli*-type and the precursor-type analogues CM-506 and CM-406 in which the phosphoryl group at the 1-position was replaced with a carboxymethyl (CM) group.[20,39] The activity of both CM-506 and CM-406 was indistinguishable from their corresponding natural-type compounds. The β-CM analogues having acidic groups β-glycosidically linked at the 1-position also showed potent activity.[21] We also synthesized two analogues that had two CM groups at 1- and 4′-positions, *E. coli*-type (Bis-CM-506) and precursor-type (Bis-CM-406), both of which showed respective activities.[40,41] The acidic functional groups are concluded to be essential,[42] but their strict type is not necessary for expression of the biological activity.

Although we had already improved the synthetic procedure for lipid A in many aspects, it still had many reaction steps and as a consequence considerable time and laborious work was required for the completion of the synthesis. In order to facilitate the synthesis, we developed a new synthetic methodology termed Synthesis based on Affinity Separation (SAS). The basic principle of SAS is as follows. A tag molecule is covalently attached to a substrate. The reactions are carried out in solutions, and the desired tagged products are rapidly isolated by solid-phase extraction using a specific affinity interaction between the tag and a ligand which is immobilized on a polymer support. So far, we have successfully used two interactions for SAS. One was an interaction of a crown ether or a podand ether tag and polymer-supported ammonium ions[43,44] and the other was the specific molecular recognition between a barbituric acid derivative and its artificial receptor which formed a tight complex with six hydrogen bonds[43b,45] (Figure 5). The versatility of SAS for glycoconjugate synthesis has already

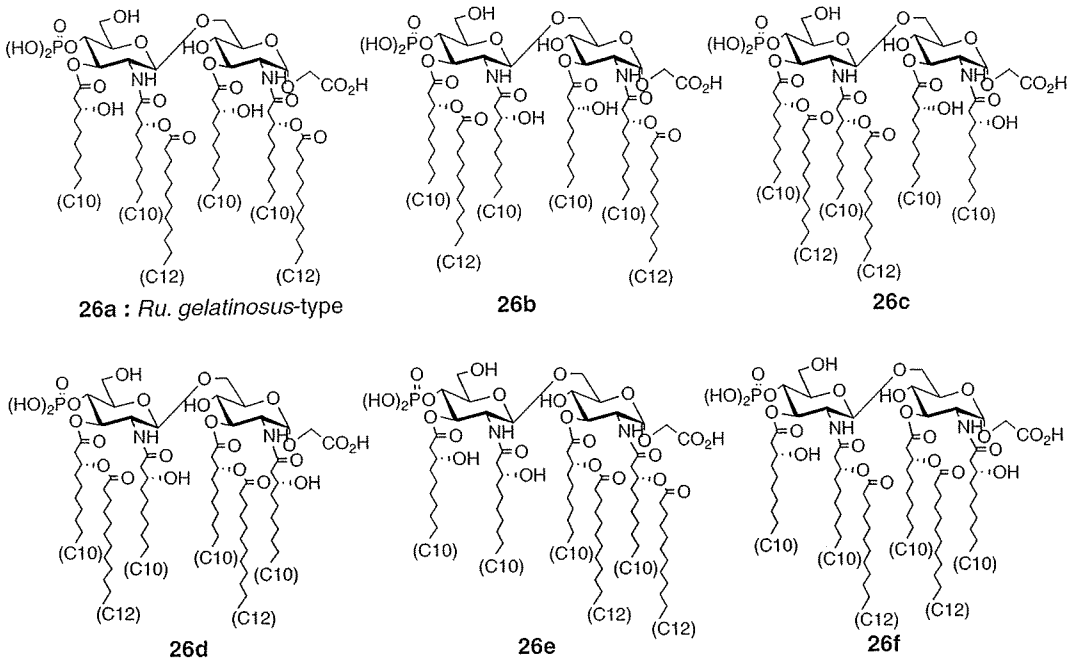

Figure 4. Lipid A library possessing six acyl groups.

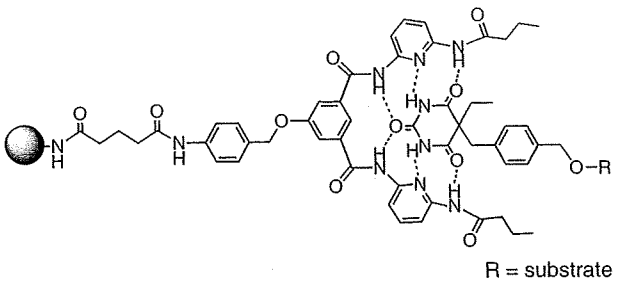

Figure 5. Host–guest interaction of a polymer-supported receptor with a barbituric acid tag.

been demonstrated by our total synthesis of *E. coli* lipid A based on the latter interaction.[31,32]

Figure 6 shows the basic synthetic route for constructing the library. A barbituric acid (BA) tag was attached to the 4-position of the glycosyl acceptor via a *p*-acylaminobenzyl linker with a glutarylamino spacer. In order to reduce the total number of reaction steps for the synthesis of the six target compounds, a $\beta(1\rightarrow6)$ disaccharide 4′-phosphate **29** was constructed as a common key synthetic intermediate by the coupling of two monosaccharides, i.e., a glycosyl trichloroacetimidate **27** as a donor and a glycosyl acceptor **28** having the BA-tag. All the acyl moieties were then introduced step by step to their respective positions. Acylation of the hydroxy group with the 3-acyloxyfatty acid in the presence of DMAP sometimes caused β-elimination of the 3-acyloxy function, especially when the hydroxy group to be acylated was sterically hindered by a neighboring long chain *N*-acyl group. Therefore, acylation of the 3- or 3′-hydroxy group with the 3-acyloxyfatty acid was carried out prior to 2- and 2′-N-acylation. After introducing the four acyl groups, simultaneous deprotection and cleavage of the linker by catalytic hydrogenolysis afforded the desired CM-analogues **26a–26f**. The divergent strategy was also employed by our previous synthesis and by Boons' synthesis.[25,26]

The glycosyl donor **27**, whose 2- and 3-positions are protected with the allyloxycarbonyl (Alloc) and propargyloxycarbonyl (Proc) groups respectively, was synthesized as shown in Scheme 3. The Proc group was stable to neat TFA, but could be readily cleaved by treatment with $Co_2(CO)_8$ and TFA via an alkyne–Co complex.[46] The Proc group could also be cleaved with Zn–AcOH, Pd^0–Et_3SiH, or $[Ir(cod)(MePh_2P)_2]PF_6$ that was activated with H_2 (Ir-complex).[46b] Since the 1-*O*-allyl group could not have been isomerized to a 1-propenyl group by the Ir-complex in the presence of the *N*-Alloc group, *N*-Fmoc glucosamine allyl glycoside **31** was used as a starting material. The allyl group was isomerized to a 1-propenyl group by using the Ir-complex before introduction of the Proc group, since the latter is readily cleaved with the Ir-complex. The 3-*O*-Proc derivative **32** formed in 94% yield was treated with 1,3,4,6,7,8-hexahydro-2*H*-pyrimido[1,2-α]-pyrimidine, polymer-bound, (PTBD) to remove the 2-*N*-Fmoc group.[47] The reaction was slow with PTBD and 1 day was required for the complete removal of the Fmoc group, but the solid base was removed by simple filtration and thus the work-up operation was quite simple. After the free 2-amino group was again protected with an Alloc group, reductive opening of the 4,6-*O*-benzylidene ring of **33** was effected by the use of the combination of Et_3SiH and $BF_3\cdot Et_2O$. In a small scale experiment (0.17 mmol of **33**), $BF_3\cdot Et_2O$ was added at once to a solution of the 4,6-O-benzylidenated compound **33** and Et_3SiH in CH_2Cl_2 at 0 °C to give the desired 6-O-benzylated product **34** in 93% yield. In a large scale (21.6 mmol of **33**), even when $BF_3\cdot Et_2O$ was added dropwisely, 30% of 3-*O*-Alloc derivative was formed by an undesired reduction of the Proc group. 4-O-Phosphination of **34** and a subsequent oxidation gave phosphate **35** in 91% yield. After removal of the 1-propenyl group with aqueous I_2, treatment with CCl_3CN and Cs_2CO_3 furnished glycosyl trichloroacetimidate **27**.